PREDICTION OF GROUND MOTION IN NORTH AMERICA

David M. Boore
William B. Joyner
Geophysicists, U. S. Geological Survey
Menlo Park, California 94025

Abstract

Because recordings of ground motion are not distributed uniformly across North America, the methods for predicting ground motions are regionally dependent. Most of the recorded ground motions are from the coastal regions of California, and for these regions empirical studies provide the basis for the prediction of ground motion for most earthquakes of engineering interest. These studies show that the response spectra depend strongly on magnitude and site conditions. This means that the scaling of a standard spectral shape by peak acceleration is a poor means of estimating spectral amplitudes. In regions away from coastal California the prediction of ground motion must use a combination of theoretical and observational studies. A particularly useful method, often called the stochastic model, was developed somewhat over ten years ago and has been widely applied in regions lacking ground-motion data from earthquakes of engineering interest. In all regions the near-surface geologic materials can strongly influence the earthquake shaking at the Earth's surface and must be accounted for.

Introduction

The design of any engineered structure is based on an estimate of ground motion, either implicitly through the use of building codes or explicitly in the site-specific design of large or particularly critical structures.

There are a number of methods for estimating ground motions, which we classify into two groups: empirical estimation, making use of previously-recorded ground motions, and estimation that uses seismological models to account for the seismic source, wave propagation en route to the site, and modifications introduced by local geologic structure. Of course, such a division is somewhat arbitrary, for the modeling studies often use empirical data to fix some of the parameters, and the empirical estimates usually are based on regression fits to a functional form suggested by theoretical considerations.

We are concerned in this paper with ground-motion estimation throughout North America. We start the paper with a short discussion of factors that affect ground motions. Specific results are then given for the empirical and theoretical models. We discuss which model is appropriate for various regions in North America; in general, the empirical model can be used to predict ground motions in coastal California, but not in central and eastern North America, where the theoretical model should be used. The theoretical model can also be used for predictions of ground motions in other regions of North America. This

paper will **not** be a comprehensive survey of ground-motion estimation, on the scale of, for example, Joyner and Boore (1988). Instead, we will concentrate on our recent work, which is applicable to ground-motion prediction from shallow earthquakes. With one exception (Boore, 1986), our previous research has not included the prediction of ground motions from subduction earthquakes such as might occur in the coastal region of the Pacific northwest. For that region, we make a few remarks and direct the reader to the literature.

Parameters Describing Ground Shaking

A number of different quantities calculated from strong-motion records may be used for purposes of seismic design. Peak acceleration is the most commonly used; other quantities used are peak velocity and response spectral values. The response spectrum is defined as the maximum responses, to a given motion, of a set of single-degree-of-freedom oscillators (for example, mass-spring systems) having different natural periods and damping. The response spectral values are useful in structural design because they take account of the frequency of the structure. The response spectrum can be thought of as the maximum responses, to a given motion, of a set of simple mathematical models of structures.

Peak horizontal acceleration may be used in simplified procedures for evaluating liquefaction potential and in pseudostatic studies of slope stability. Peak acceleration has also been commonly used in the past as a scaling parameter to scale a normalized spectral shape and obtain response spectra for analysis of structural response. This is an unsound procedure. It would be valid in general only if the shape of response spectra were independent of earthquake magnitude, source distance, and recording-site conditions. A number of studies (McGuire, 1974; Mohraz, 1976; Trifunac and Anderson, 1978; Joyner and Boore, 1982; Boore *et al.*, 1993), however, have shown that the shapes of response spectra are strongly dependent on magnitude and site conditions. Since long-period ground motion increases with magnitude more than peak acceleration, scaling some sort of average spectral shape by peak acceleration will seriously underestimate long-period motions at large magnitude. At periods greater than about 0.3 sec, large errors can result from the practice of scaling by peak acceleration. These errors can be partially avoided by Newmark and Hall's (1982) method, in which the spectrum at short-periods, intermediate periods (about 0.3 to 2.0 sec), and long periods is derived by applying a scaling factor to peak acceleration, peak velocity, and peak displacement, respectively. Our work, however, shows that the proportionality factor between velocity and intermediate-period response varies significantly with magnitude and site conditions and that the shape of the response spectrum varies significantly with distance; furthermore, the proportionality factors at short periods may not be appropriate for earthquakes in eastern North America. We prefer to estimate response spectra directly, either by regression of individual spectral ordinates for a suite of periods or by using the theoretical model to be described later. One point deserves emphasis: the search for a single parameter to characterize ground motion is doomed to failure. Because the shape of the spectrum changes with magnitude and site conditions, a single parameter that represents ground motion well at one period must necessarily fail to do so at others.

Explanatory Variables

Magnitude

Earthquake ground motions depend on the size of the earthquake, the most common measure of which is magnitude. Reduced to their essence, conventional measures of magnitude are defined in terms of peak motions observed on seismograms from particular instruments after correction for attenuation to a reference distance. The waves radiated from an earthquake are made up of a wide spectrum of frequencies, and seismic instruments provide views into different frequency windows of the radiated energy (some emphasize long-period motions, while others respond to higher-frequency shaking). Because of this, the size of any earthquake can be measured by a number of magnitude scales. There is no guarantee that the magnitudes for any earthquake will agree with one another (nor, according to seismological models of the source, should they be expected to). While confusing, it must be remembered that each scale provides information about the spectral excitation of the source at different frequencies. The most commonly used magnitudes in engineering design are the Richter local magnitude M_L, the short-period magnitude m_{bLg}, the surface-wave magnitude M_S, and the moment magnitude M.

M_L is determined from the trace amplitude on a record made by a particular kind of seismograph, the Wood-Anderson seismograph, located within a few hundred km of the earthquake, and is used primarily in California. m_{bLg} is a short-period magnitude scale commonly used in North America east of the tectonic areas of western North America. It is measured from peak motions recorded at distances up to a thousand kilometers on instruments with a passband generally in the 1 to 10 Hz range. The peak motions from these instruments usually correspond to the Lg wave, a relatively slowly-traveling wave made up of P and S waves reverberating in the earth's crust. M_S is determined from the ground motion associated with surface waves of 20 s period recorded anywhere in the world. The moment magnitude, M, is measured from the energy radiated from the source at periods long enough so that all of the higher-frequency complexity of the source is smoothed out. Obtaining M for an earthquake is not as straightforward as it is for m_{bLg}. The moment-magnitude scale, first explicitly described by Hanks and Kanamori (1979), is related to the seismic moment of the fault through the simple relation $\mathrm{M} = (2/3)\log M_0 - 10.7$; the seismic moment M_0, which controls the amplitude of long-period seismic waves, is the product of the average slip across the fault surface, the area of the fault surface, and the modulus of rigidity (or the shear modulus) of the rocks surrounding the fault.

As stated before, a number of magnitudes can be measured for a given earthquake. By combining data from many earthquakes (and, as discussed later, by using theoretical calculations in the case of m_{bLg}), empirical relations between the magnitude scales can be obtained. Relations obtained in this way for M_L, m_{bLg}, and M_S as a function of M are shown in Figure 1. Each of these magnitudes is numerically equal to moment magnitude over only a limited range of magnitude. The nonlinear relations between the magnitude scales is a potential source of confusion and bias in ground-motion prediction, and it is

essential in engineering practice that the magnitude scale being used be clearly stated. We recommend the use of moment magnitude M. It corresponds to a well-defined physical property of the earthquake source, and is thus a measure of the size of an earthquake in a very specific sense. Use of moment magnitude has the advantage of making it easier to relate earthquake occurrence rates to geologically determined fault slip rates (e.g., Joyner and Fumal, 1985). It is sometimes stated that because M_L and m_{bLg} are determined from instruments with a natural periods in the period range of greatest engineering interest, they should be preferred as the measure of earthquake size to use in making ground-motion estimates for engineering purposes. Catalog values of M_L and m_{bLg} for large earthquakes, however, are commonly poorly determined, and moment magnitude is the better measure for such use.

Another argument in favor of a short-period magnitude scale in eastern and central North America is that regional catalogs of earthquake seismicity usually use m_{bLg} as the measure of earthquake size, and therefore estimates of seismicity and design earthquakes are specified in terms of m_{bLg}. Recent methods of ground-motion estimation, on the other hand, use M as the fundamental measure of source strength. It is possible to redo the earthquake catalogs in terms of M by using correlations between M and areas enclosed by contours of equal intensity (Hanks and Johnston, 1992). We recommend that this be done, but until then a relation must be established between m_{bLg} and M. There are not enough data to establish such a relation, particularly for large earthquakes. The available data are shown in Figure 2, where the squares outline the range of magnitudes published for individual earthquakes, and the filled circles are the magnitudes preferred by the first author of this paper. Overall, there is a good correlation between the two magnitudes. Some of the scatter is due to real differences in the relative amounts of energy radiated at high- and low-frequencies, and some of the scatter is observational error due to limited available data (this is particularly true for the older earthquakes which control the correlation at high magnitudes). The data suggest a linear relation between m_{bLg} and M. On the other hand, model calculations indicate that the relation should have curvature in the sense that there is less increase in the high-frequency magnitude (m_{bLg}) for a given increase in the low-frequency magnitude (M) for large earthquakes. The relation shown in Figure 1 (which is the same as the solid curve in Figure 2) came from fitting a polynomial to simulated pairs of m_{bLg} and M points, computed by using the stochastic model described later in this chapter.

Distance

Because the rupture surface for earthquakes may extend over tens or hundreds of kilometers, there is ambiguity in defining the source distance for a strong-motion record. Various measures of source distance have been used in the development of relationships for estimating ground motion. Some of these are illustrated in Figure 3. The early analyses tended to use epicentral distance because it was readily available. Obvious problems arise with the use of either epicentral or hypocentral distance in the case of earthquakes like the 1966 Parkfield, California, earthquake or the 1979 Imperial Valley, California, earthquake, which have very long rupture zones with the epicenter at one end and recording stations

at the other. For some stations the epicenter and hypocenter are many times more distant than the closer portions of the rupture which are in fact the sources of the peak motions. Similar problems arise with the use of distance to the centroid of the rupture. Some stations may be far from the centroid but close to the rupture. In general it must be expected that different parts of the fault rupture will produce the peak motion at different recording stations. It might seem that the distance measure to use is the distance to the part of the rupture producing the peak motion. Where that part of the rupture is located, however, is unknown for many past earthquakes and for all future earthquakes. Most recent work has used some variation on the closest distance to the rupture. We used the closest distance to the point on the Earth's surface directly above the ruptured part of the fault (Joyner and Boore, 1981, 1982; Boore *et al.*, 1993).

Site Conditions

It is well known that geologic conditions near the Earth's surface can produce large effects on ground shaking. In many applications the site effect is calculated on a site-specific basis; we will not review the methods for doing so here. A more general accounting for site effects can also be useful, particularly if the predicted motions are for a general class of sites rather than a specific site. In this case, a number of schemes have been used for grouping local sites into a few categories. Some of the groupings are based on descriptive terms (e.g., "rock" and "soil"), while others have a more quantitative basis. We have recently used the time-weighted average of the shear-wave velocity from the surface to a depth of 30 m as the basis for grouping sites into four classes, following the grouping proposed for the 1994 edition of the National Earthquake Hazard Reduction Program's recommended code provisions. We have also developed equations for site-specific ground-motion predictions, again using the shear velocity averaged over the uppermost 30 m.

Shallow Earthquakes in Western North America

Ideally, a sufficient number of recordings of ground motion near a site would be available to allow a direct empirical estimation of the motions expected for a design earthquake. This is rarely possible, as there are simply too few recordings available. Because large earthquakes are relatively rare events and the funding for strong-motion instrumentation is limited, the number of available records is small, particularly for large magnitudes and small source distances, just the conditions most critical for earthquake-resistant design. On the positive side, there are hundreds of ground-motion recordings in western North America for shallow earthquakes, a fortunate situation not shared by other regions of North America. For example, Figure 4 shows the magnitude and distance distribution of recordings used in our recent derivation of prediction equations (Boore *et al.*, 1993). The method for predicting ground motions in western North America (and more specifically, coastal California) is to fit equations or graphical curves to these data, with explanatory variables that include magnitude, distance, and some measure of site condition. A number of different relationships for estimating ground motion have been developed. A comprehensive review of relationships developed before the 1979 Imperial Valley, California, earthquake is given by Idriss (1979). The 1979 Imperial Valley

earthquake marked a major change in the strong-motion data base by providing many more near-source data points than had been available previously. More recent reviews have been written by us (Boore and Joyner, 1982; Joyner and Boore, 1988) and Campbell (1985).

Results for Site Classes

We have recently revised our equations for estimating horizontal ground motion from shallow earthquakes in western North America. In doing this, we classified the sites into groups A, B, C, and D, depending on their shear velocity. The grouping is given in Table 1. The functional form of the equations is given by:

$$\begin{aligned} \log Y =& b_1 + b_2(\mathrm{M}-6) + b_3(\mathrm{M}-6)^2 + b_4 r + b_5 \log r + b_6 G_B + b_7 G_C \\ & 5.0 \le \mathrm{M} \le 7.7 \\ & r = (d^2 + h^2)^{1/2} \end{aligned} \tag{1}$$

where Y is the ground-motion quantity to be estimated, M is the moment magnitude of the earthquake, d is the shortest distance (km) from the site of interest to the point on the Earth's surface directly over the fault rupture, and $G_B = 1$ and $G_C = 1$ for site classes B and C, respectively, and are zero otherwise (group D is poorly represented in the data set and was not included in the regression analysis). The values of the coefficients are given in Boore *et al.* (1993).

The results for site class C as a function of distance are shown in Figure 5. Note that the sensitivity to magnitude is greater for long-period response spectra than it is for peak acceleration and short-period response spectra, a finding consistent with previous studies and expected from seismological models of source scaling. Note also that curves for each magnitude have the same shape. This is imposed by our choice of the functional form (equation (1)), and is in contrast to the assumed shape in several other studies. Studies of residuals of the data with respect to our curves gives us no reason for introducing additional parameters to allow the shape of the curves to be magnitude dependent.

The dependence on magnitude is also given in Figure 6, which shows acceleration response as a function of period for a fixed distance. Clearly, the shape of the response spectrum is a strong function of magnitude, reinforcing the conclusion found in earlier studies that it is inadvisable to construct a design spectrum by simply scaling a fixed spectral shape.

The response spectra are strongly dependent on site class, as shown in Figure 7. Although not easy to see on the linear scale used in the figure, the amplification of sites B and C relative to class A increases with oscillator period; it is more than a factor of 3 for class C sites at periods greater than 1 sec. The dependence on site also exists at the shortest periods in our analysis.

It is important to study the residuals of the data relative to the predictions in order to reveal any biases in the prediction equations that might be due to the particular functional

form assumed in the analysis. We have done that, with the residuals for peak acceleration shown as an example in Figure 8. We see no persistent trends in the residuals, indicating that our equations provide a good approximation to the observations when averaged over all events and distances. As we will show later, this is not to say that the data from any particular event could not have systematic departures from the predicted motions (which are intended to represent median motions averaged over the population of earthquakes of a specified size and distance).

Results for Continuous Velocity Variation

Even though the classification system used in the previous section is an improvement over older classification schemes based on qualitative descriptions of site geology, it would be better still to compute the site effect as a continuous function of shear-wave velocity, if available. We have done that, generally following the ideas of Joyner and Fumal (1984). The term

$$b_V(\log V_S - \log V_A) \tag{2}$$

replaces the term

$$b_6 G_B + b_7 G_C$$

in equation (1), where V_S is the time-averaged velocity at a site, and b_V and V_A are parameters determined from regression analysis. The values of the coefficients for different oscillator periods and dampings are given in Boore *et al.* (1994). The amplification given by equation (2) is shown in Figure 9 for a set of eight oscillator periods uniformly distributed logarithmically between 0.1 and 2 seconds. The plots show strong correlation of long-period ground motion with shear-wave velocity, consistent with the results when discrete classes are used to describe the geologic conditions at sites.

The dependence of the amplification on shear velocity is given by the coefficient b_V in equation (2); it was determined from earthquakes in California. As shown in Figure 10, the velocity dependence is remarkably similar to that determined by Midorikawa (written comm., 1993) in Japan and to the coefficients proposed by Borcherdt (1994) for use in determining short- and mid-period amplification factors in building codes.

Comparison of Results with Data from Specific Earthquakes

The peak acceleration predicted by the equations of Boore *et al.* (1993) are compared to the data from the 1989 Loma Prieta earthquake in Figure 11. The figure shows that there is a well-defined dependence of the peak accelerations on site class (this is the first earthquake clearly to show this effect). Also note that, on the average, the observed accelerations are consistently above the predicted values for each site class. This is not a troubling result, for the predictions are for the median value of a whole population of events with a magnitude equal to that of the Loma Prieta earthquake; we would expect some of the events to have values consistently above the predicted values and some to have values that are consistently lower than the predictions.

There is a suggestion that the distance-dependence of the data is not the monotonic decay of the predicted motions, although the scatter in the data makes it difficult to be certain of this point. In particular, as pointed out by P. Somerville and colleagues (e.g., Burger *et al.*, 1987; Somerville and Yoshimura, 1990), the curvature of the rays traveling through the Earth's crust and reflections from the layers within the Earth (particularly the Mohorovičić discontinuity) should produce a decay at short distance more rapid than inverse distance, followed by a flattening or an increase of amplitude in the 50 to 100 km distance range (depending on earthquake depth, crustal thickness, and velocity contrast at the discontinuity). The recordings of the mainshock may be too sparse along any given path to show clearly these effects, but this is not true of aftershock recordings made on portable instruments installed after the mainshock. Figure 12 shows the distance attenuation determined by Fletcher and Boatwright (1991) for a line extending from the source region to San Francisco. Their study shows the expected variations relative to simple inverse-distance geometrical spreading.

Comparable comparisons to the Loma Prieta data are shown in Figures 13 and 14 for recordings of the 1992 Landers main- and aftershocks, and similar remarks apply. As found by Mori (1993), the distance variation of the Landers aftershock data are strongly dependent on the path traversed from the source to the station. This dependence on path (presumably due to differences in crustal structure) may explain why the residuals of the data relative to the predicted attenuation from the analysis by Boore *et al.* (1993) of many earthquakes in western North America do not show the more complicated character expected for motions traversing a single path; these effects are averaged out. The Landers aftershock data also indicate that a substantial portion of the scatter in the strong-motion data about the mean predictions can be due to variations in crustal structure.

A comparison of the attenuation of motions from both the Loma Prieta and the Landers earthquakes is shown in Figure 15. An arbitrary vertical adjustment of the data was applied such that the two data sets approximately coincide at 40 km. If this is a valid normalization, the figure shows that the attenuation of motions along the San Francisco Peninsula from a source to the south is similar to that along a path from the Landers aftershock area to station GSC.

Subduction Earthquakes in the Pacific Northwest

A number of studies have estimated ground motions from earthquakes in the Pacific Northwest. These include Langston (1981), Heaton and Hartzell (1986), Ihnen and Hadley (1986), Youngs *et al.* (1988), Heaton and Hartzell (1989), Silva and Darragh (1989), Wong and Silva (1990), Cohee *et al.* (1991), Crouse (1991), and Wong *et al.* (1993).

In evaluating the published studies, it must be noted that some regression studies of data from Japanese earthquakes found the attenuation of motion with distance to be much less rapid than found for shallow earthquakes in western North America. Fukushima and Tanaka (1990), however, showed that these results were caused by use of unweighted least-squares regression. A properly weighted regression analysis applied to the same data found

that the distance attenuation was similar to that from shallow western North American earthquakes.

Earthquakes in Central and Eastern North America

Basis of Predictions

In many regions, such as central and eastern North America (which, for convenience, we refer to as "CENA"), too few strong-motion data are available for making empirical estimates. This is clearly shown in Figure 16, which plots a symbol for each recording as a function of magnitude and distance. Comparison of Figure 16 with the plot for western North America (Figure 4) shows that in CENA there are many fewer data in the critical range of earthquakes with magnitudes greater than 5, at distances less than 200 km. To emphasize the point, shaded lines have been added to Figure 16 to indicate the range of magnitudes and distances in Figure 4. Why not estimate ground motion theoretically? The theory of seismic wave propagation is sufficiently well developed so that ground motion could be calculated *if* all the necessary information were available. The catch is that the needed information is not available, and, in our view, probably will not be within the foreseeable future, if ever. The fault rupture that is the source of ground motion may be 10 km or more beneath the surface of the earth. It would be necessary to know the properties of all the material along the propagation path between the fault at depth and the site on the surface where the ground-motion estimate was wanted. The amount of slip on the fault would have to be known, and, more importantly, how that slip varied from point-to-point on the fault. A new approach has been developed recently, however, that makes theoretical estimates of earthquake ground motion possible. It combines simple approximations to wave-propagation effects with a statistical description of the variability of slip on the fault. Estimates made with this approach agree very well with the recorded ground-motion data that is available, and the approach makes possible what, in our view, are the first realistic theoretical estimates in regions for which there are few data.

The model is usually referred to as the stochastic model. The model was first proposed by Hanks and McGuire (1981) and was later developed by several authors (e.g., Boore, 1983; Boore and Joyner, 1984; Toro and McGuire, 1987). The essence of the stochastic model is shown in Figure 17. The energy radiated from an earthquake is assumed to be distributed randomly over a time interval determined by the source duration prolonged by arrivals from multiple travel paths. The idea that the motions are random has been used for years by engineers as a basis for their derivation of design motions; the crucial difference in the stochastic model is that the spectral content of the motions is given by seismological models, and therefore there is a physical and observational basis for the amplitude and relative frequency content of the motions. Extrapolations to situations lacking empirical data can be made with more confidence than is the case with previous models based on random processes. The model is very flexible and can be readily modified to incorporate various source-scaling relations, path effects, or site effects. It has the benefit that the computations are very rapid, and the sensitivity of motion to input parameters can be easily tested. The model is not limited in its application to CENA. The model has been verified

by comparison with world-wide data over a wide range of magnitudes and frequencies (e.g., Boore, 1983, 1986a,b). The model was first applied to CENA ground-motion estimation by Atkinson (1984), who used it to predict peak acceleration and velocity on hard-rock sites. Boore and Atkinson (1987) and Toro and McGuire (1987) extended the model to the estimation of response spectra, and Boore and Joyner (1991) included the effect of deep soil on ground motion. The stochastic-model-based attenuation equations published in 1987 by Boore and Atkinson and by Toro and McGuire are currently being revised by those authors. Other applications include those of Chapman *et al.* (1990), Campbell (1991), and Toro *et al.* (1992). In addition, many of the applications of the stochastic model to ENA have been made by large projects directed by the Electric Power Research Institute and by the Lawrence Livermore Laboratory; much of that work has not been published (but see Toro *et al.*, 1988, and Bernreuter *et al.*, 1989).

In applications to CENA, there is a parameter with units of stress (usually symbolized as $\Delta\sigma$; see Boore, 1983, for more explanation) that has a direct influence on ground motion, particularly at the periods of most concern to engineers. The sensitivity of ground motions to this parameter is shown in Figure 18. Unfortunately, $\Delta\sigma$ is perhaps the least well constrained of the important model parameters. Estimates of this parameter for CENA earthquakes range from less than 50 to over 400 bars, with a median value near 150 bars (Atkinson, 1993). This variation gives rise to considerable random variation of individual ground motions about the median values.

There is some indication that the median value of $\Delta\sigma$ is larger in CENA than in western North America. Another model parameter that seems to be different in the two regions is the parameter controlling the attenuation of seismic energy at high frequencies (this is modeled in Figure 17 by a high-frequency corner beyond which the spectral amplitudes decrease rapidly). The rock underlying sites in western North America is commonly highly fractured and deeply weathered. In contrast, rock sites in eastern North America (particularly those areas that were overridden by glaciers during the Pleistocene epoch) are typically very hard, with little weathering and few fractures. This difference shows up in CENA earthquakes at hard-rock sites having much more short-period motion at distances close to the source than western North American earthquakes. An example of this is shown in Figure 19. The acceleration spectra have been normalized to unity at a period of 0.3 sec to account for the difference in magnitude of the events (4.0 for Miramichi and 5.3 for Daly City); both recordings were obtained within 10 km of the earthquake source. The Daly City acceleration spectra have peaks in the period range of 0.1 to 0.3 sec, but the peak for the Miramichi recording occurs at a period smaller than 0.05 sec.

Application to Rock Sites

Some of the results from an application of the stochastic model to prediction of ground motions at hard-rock sites in CENA have already been presented in Figure 18. Further results are contained in Figure 20, which shows the attenuation of various ground-motion measures as a function of distance for a suite of magnitudes. Note that the separation

between the curves is greater for low-frequency than for high-frequency oscillators or for peak acceleration, just as it is for the empirical results for western North America (Figure 6). This difference in magnitude scaling is a direct consequence of the seismological source model shown in Figure 17: the difference of 2 units in moment magnitude (5 to 7) requires that the source spectra differ by 3 orders of magnitude at very low frequency and that the corner frequencies (f_o in the figure) differ by a factor of 10. Purely geometric considerations then lead to a smaller difference between the curves at frequencies above the corner frequencies f_o.

Application to Soil Sites

Not all of CENA is underlain by hard rock at the surface, and for those sites the lower-velocity near-surface sediments must be accounted for in the predictions of ground motion. This can be done using site-specific studies or by deriving correction factors for generic soil profiles. Figure 21 shows a compilation of shear-velocity profiles from a number of deep-soil sites, with an average profile indicated by the heavy line. Boore and Joyner (1991) derived correction factors for this profile and published equations from which deep-soil ground motions in CENA can be obtained. Figure 22 shows that correction factor (the factor that has to be added to the logarithm of the response spectral values on rock) for Boore and Joyner's generic soil, and for two site-specific soil profiles. The predictions of response spectra on soil and rock are shown in Figure 23.

Comparison of Ground Motions in Western and Eastern North America

A comparison of ground motions on rock sites in western and CENA predicted from methods discussed in this paper is shown in Figure 24. Note the large difference in the response amplitudes at short periods, similar to that seen in the comparison of spectra from the Daly City and Miramichi recordings (Figure 19).

The difference in short-period content manifests itself in another way. Response spectra calculated using Newmark and Hall's scheme (Newmark and Hall, 1982) in which peak displacement, velocity, and acceleration are multiplied by amplification factors may not result in enough short-period response; an example of this is shown in Figure 25. The source of the problem is that the amplification factors are based on western North American earthquakes, but as we have shown, ground motions at close distances to earthquakes in CENA can be much richer in short-period energy.

Acknowledgments

We thank Jack Boatwright, S. Midorikawa, and Jim Mori for data and curves, Walt Silva for the site-specific correction factors shown in Figure 22, and Linda Seekins for providing a thorough review. This work was partially funded by the U. S. Nuclear Regulatory Commission.

References

Atkinson, G. M. (1984). Attenuation of strong ground motion in Canada from a random vibrations approach, *Bull. Seism. Soc. Am.* **74**, 2629–2653.

Atkinson, G. M. (1993). Earthquake source spectra in eastern North America, *Bull. Seism. Soc. Am.* **83**, 1778–1798.

Atkinson, G. M. and D. M. Boore (1987). On the m_N, M relation for eastern North American earthquakes, *Seism. Res. Lett.* **58**, 119–124.

Bernreuter, D. L., J. B. Savy, R. W. Mensing, and J. C. Chen (1989). Seismic Hazard Characterization of 69 Nuclear Plant Sites East of the Rocky Mountains, *U.S. Nuclear Regulatory Commission Report NUREG/CR-5200*, Lawrence Livermore National Laboratory Report UCID-21517, Vol. 7.

Boore, D. M. (1983). Stochastic simulation of high-frequency ground motions based on seismological models of the radiated spectra, *Bull. Seism. Soc. Am.* **73**, 1865–1894.

Boore, D. M. (1986a). Short-period P- and S-Wave radiation from large earthquakes: Implications for spectral scaling relations, *Bull. Seism. Soc. Am.* **76**, 43–64.

Boore, D. M. (1986b). The effect of finite bandwidth on seismic scaling relationships, in *Earthquake Source Mechanics*, S. Das, J. Boatwright, and C. Scholz, Editors, Geophysical Monograph 37, American Geophysical Union, Washington, D. C., 275–283.

Boore, D. M. (1989). Quantitative ground-motion estimates, in *Earthquake Hazards and the Design of Constructed Facilities in the Eastern United States*, K. H. Jacob and C. J. Turkstra, Eds., Annals of the New York Academy of Sciences, Vol. 558, 81–94.

Boore, D. M., and G. M. Atkinson (1987). Stochastic prediction of ground motion and spectral response parameters at hard-rock sites in eastern North America, *Bull. Seism. Soc. Am.* **77**, 440–467.

Boore, D. M. and W. B. Joyner (1982). The empirical prediction of ground motion, *Bull. Seism. Soc. Am.* **72**, S43–S60.

Boore, D. M. and W. B. Joyner (1984). A note on the use of random vibration theory to predict peak amplitudes of transient signals, *Bull. Seism. Soc. Am.* **74**, 2035–2039.

Boore, D. M., and W. B. Joyner (1991). Estimation of ground motion at deep soil sites in eastern North America, *Bull. Seism. Soc. Am.* **81**, 2167–2185.

Boore, D. M., W. B. Joyner, and T. E. Fumal (1993). Estimation of response spectra and peak accelerations from western North American earthquakes: An interim report, *U. S. Geol. Surv. Open-File Rept. 93-509*, 72 pp.

Boore, D. M., W. B. Joyner, and T. E. Fumal (1994). Estimation of response spectra and peak accelerations from western North American earthquakes: An interim report, Part Two, *U. S. Geol. Surv. Open-File Rept.* , (in press).

Borcherdt, R. D. (1994). Simplified site classes and empirical amplification factors for site-dependent code provisions, it Proceedings NCEER, SEAOC, BSSC Workshop on Site Response During Earthquakes and Seismic Code Provisions, *University of Southern California, November 18-20, 1992*, (in press).

Burger, R. W., P. G. Somerville, J. S. Barker, R. B. Herrmann, and D. V. Helmberger (1987). The effect of crustal structure on strong ground motion attenuation relations in eastern North America, *Bull. Seism. Soc. Am.* **77**, 420–439.

Campbell, K. W. (1985). Strong motion attenuation relations: A ten-year perspective, *Earthquake Spectra* **1**, 759–804.

Campbell, K. W. (1991). The effect of anelastic attenuation on the attenuation of peak strong-motion parameters and response spectra (abstract), *Seism. Res. Lett.* **62**, 48.

Chapman, M. C., G. A. Bollinger, M. S. Sibol, and D. E. Stephenson (1990). The influence of the coastal plain sedimentary wedge on strong ground motions from the 1886 Charleston, South Carolina, earthquake, *Earthquake Spectra* **6**, 617–640.

Cohee, B. P., P. G. Somerville, and N. A. Abrahamson (1991). Simulated ground motions for hypothesized $M_w = 8$ subduction earthquakes in Washington and Oregon, *Bull. Seism. Soc. Am.* **81**, 28–56.

Crouse, C. B. (1991). Ground motion attenuation equations for earthquakes on the Cascadia subduction zone, *Earthquake Spectra* **7**, 201–236.

Ekström, G. A. (1987). A broad band method of earthquake analysis, **Ph. D. thesis**, *Harvard University, Harvard, MA*

Fletcher, J. B. and J. Boatwright (1991). Source parameters of Loma Prieta aftershocks and wave propagation characteristics along the San Francisco Peninsula from a joint inversion of digital seismograms, *Bull. Seism. Soc. Am.* **81**, 1783–1812.

Fukushima, Y. and T. Tanaka (1990). A new attenuation relation for peak horizontal acceleration of strong earthquake ground motion in Japan, *Bull. Seism. Soc. Am.* **80**, 757–783.

Hanks, T. C. and D. M. Boore (1984). Moment-magnitude relations in theory and practice, *J. Geophys. Res.* **89**, 6229–6235.

Hanks, T. C. and A. C. Johnston (1992). Common features of the excitation and propagation of strong ground motion for North American earthquakes, *Bull. Seism. Soc. Am.* **82**, 1–23.

Hanks, T. C. and H. Kanamori (1979). A moment magnitude scale, *J. Geophys. Res.* **84**, 2348–2350.

Hanks, T. C. and R. K. McGuire (1981). The character of high frequency strong ground motion, *Bull. Seism. Soc. Am.* **71**, 2071–2095.

Heaton, T. H., and S. H. Hartzell (1986). Estimation of strong ground motions from hypothetical earthquakes on the Cascadia subduction zone, Pacific Northwest, *U.S. Geol. Surv. Open-File Rep. 86-328*, 40 p.

Heaton, T. H., and S. H. Hartzell (1989). Estimation of strong ground motions for hypothetical earthquakes on the Cascadia subduction zone, Pacific Northwest, *Pure Applied Geophysics.* **129**, 131–201.

Idriss, I. M. (1979). Characteristics of earthquake ground motions, in *Earthquake Engineering and Soil Dynamics, Proc. Am. Soc. Civil Eng. Geotech. Eng. Div. Specialty Conf.*, June 19–21, 1978, Pasadena, California, **3**, 1151–1265.

Ihnen, S. M. and D. M. Hadley (1986). Prediction of strong ground motion in the Puget Sound region: The 1965 Seattle earthquake, *Bull. Seism. Soc. Am.* **76**, 905–922.

Joyner, W.B. and D.M. Boore (1981). Peak acceleration and velocity from strong-motion records including records from the 1979 Imperial Valley, California, earthquake, *Bull. Seism. Soc. Am.* **71**, 2011–2038.

Joyner, W.B. and D.M. Boore (1982). Prediction of earthquake response spectra, *U. S. Geol. Surv. Open-File Rept. 82-977*, 16 p.

Joyner, W.B. and D.M. Boore (1988). Measurement, characterization, and prediction of strong ground motion, in *Proc. Conf. on Earthquake Eng. and Soil Dynamics II*, GT Div/ASCE, Park City, Utah, 27–30 June 1988; 43–102.

Joyner, W. B. and T. E. Fumal (1984). Use of measured shear-wave velocity for predicting geologic site effects on strong ground motion, *Proc. Eighth World Conf. on Earthquake Eng. (San Francisco)* **2**, 777–783.

Joyner, W. B. and T. E. Fumal (1985). Predictive mapping of earthquake ground motion, in *Evaluating Earthquake Hazards in the Los Angeles Region*, J. I. Ziony, Editor, *U.S.*

Geol. Surv. Profess. Paper 1360, 203–220.

Langston, C. A. (1981). A study of Puget Sound strong ground motion, *Bull. Seism. Soc. Am.* **71**, 883–903.

McGuire, R. K. (1974). Seismic structural response risk analysis, incorporating peak response regressions on earthquake magnitude and distance, *Research Report R74-51*, Dept. Civil Eng., Mass. Inst. of Tech., Cambridge, Mass., 371 p.

Mohraz, B. (1976). A study of earthquake response spectra for different geological conditions, *Bull. Seism. Soc. Am.* **66**, 915–935.

Mori, J. (1993). PmP and SmS on event record sections of Landers aftershocks (abs), Program and Abstracts of 1993 Fall meeting of the American Geophysical Union, 422.

Newmark, N. M. and W. J. Hall (1982). *Earthquake Spectra and Design*, Earthquake Engineering Research Institute Monograph, 103 p.

Shakal, A. F. and D. L. Bernreuter (1981). Empirical analyses of near-source ground motion, *U.S. Nuclear Regulatory Commission Report NUREG/CR-2095.*

Somerville, P. and J. Yoshimura (1990). The influence of critical Moho reflections on strong ground motions recorded in San Francisco and Oakland during the 1989 Loma Prieta earthquake, *Geophys. Res. Lett.* **17**, 1203–1206.

Street, R., A. Zekulin, and M. Mann (1987). Free-field particle velocity recordings of the January 31, 1986 northeastern Ohio earthquake, *Seism. Res. Lett.* **58**, 111–117.

Street, R., A. Zekulin, D. Jones, and G. Min (1988). A preliminary report on the variability in particle velocity recordings of the June 10, 1987 southeastern Illinois earthquake, *Seism. Res. Lett.* **59**, 91–97.

Toro, G. R. and R. K. McGuire (1987). An investigation into earthquake ground motion characteristics in eastern North America, *Bull. Seism. Soc. Am.* **77**, 468–489.

Toro, G. R., R. K. McGuire, and W. J. Silva (1988). Engineering Model of Earthquake Ground Motion for Eastern North America, *Electric Power Research Institute, Palo Alto, Calif., Rept. No. RP-6074.*

Toro, G. R., W. J. Silva, R. K. McGuire, and R. B. Herrmann (1992). Probabilistic seismic hazard mapping of the Mississippi embayment, *Seism. Res. Lett.* **63**, 449–475.

Trifunac, M. D. and J. G. Anderson (1978). Preliminary empirical models for scaling pseudo relative velocity spectra, appendix A in *Methods for Prediction of Strong*

Earthquake Ground Motion, U.S. Nuclear Regulatory Commission Report NUREG/CR-0689, A1–A90.

Wong, I. G. and W. J. Silva (1990). Preliminary assessment of potential strong earthquake ground shaking in the Portland, Oregon, metropolitan area, *Oregon Geology* **52**, 131–134.

Wong, I. G., W. J. Silva, and I. P. Madin (1993). Strong ground shaking in the Portland, Oregon, metropolitan area: Evaluating the effects of local crustal and Cascadia subduction zone earthquakes and near-surface geology, *Oregon Geology* **55**, 137–143.

Youngs, R. R., S. M. Day, and J. L. Stevens (1988). Near field ground motions on rock for large subduction earthquakes, in *Proc. Conf. on Earthquake Eng. and Soil Dynamics II*, GT Div/ASCE, Park City, Utah, 27–30 June 1988; 445–462.

Table 1. Definition of site class

SITE CLASS	RANGE OF SHEAR VELOCITIES*
A	greater than 750 m/s
B	360 m/s to 750 m/s
C	180 m/s to 360 m/s
D	less than 180 m/s

* Shear velocity is time-averaged over the upper 30 m, computed by dividing 30 m by the travel time to 30 m.

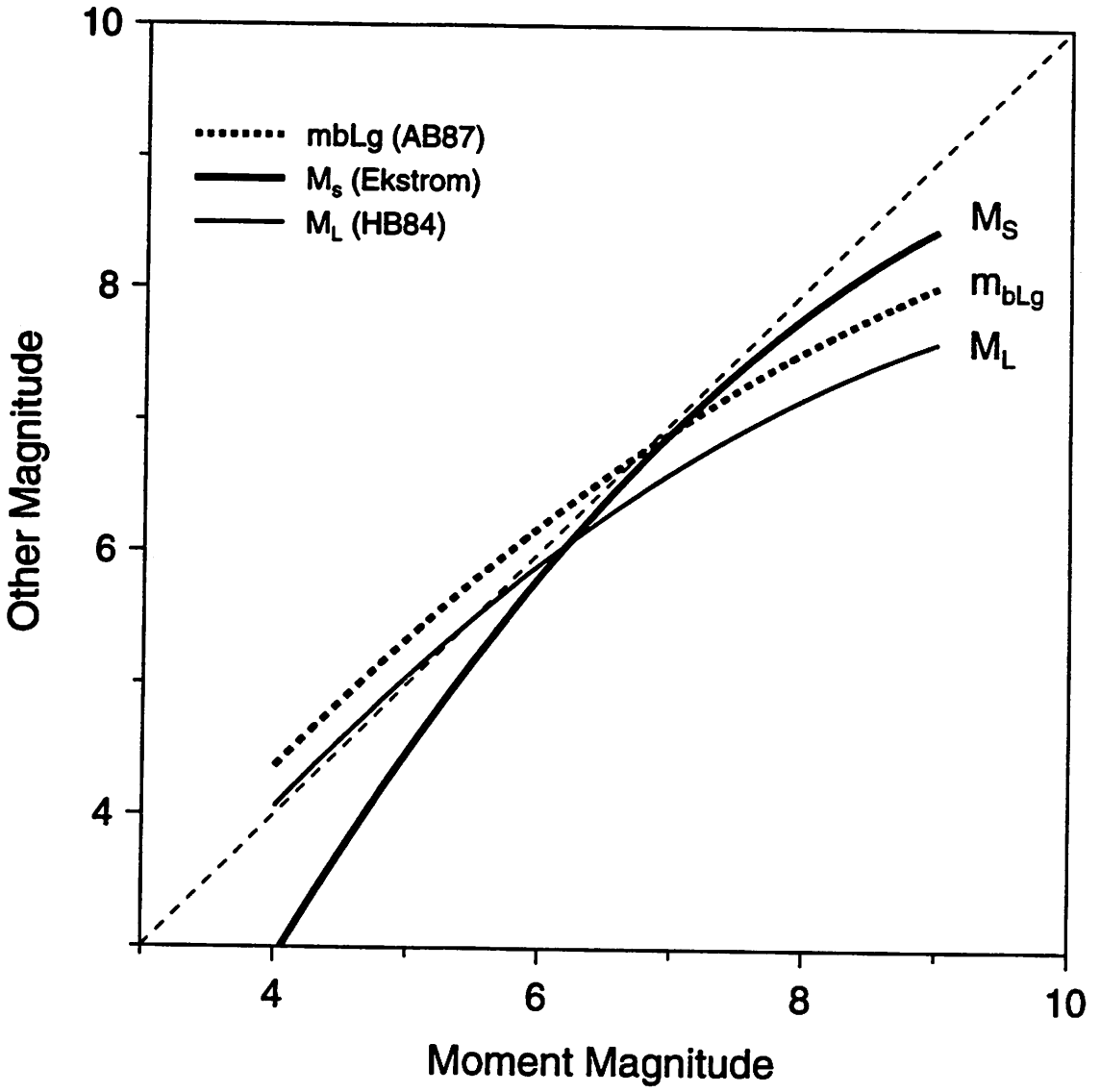

Figure 1. The functional dependence of various magnitudes on moment magnitude. The relation for m_{bLg} comes from Atkinson and Boore (1987). For M_S and M_L the relations came from fitting a quadratic to the data compiled by Ekström (1987) and Hanks and Boore (1984), respectively.

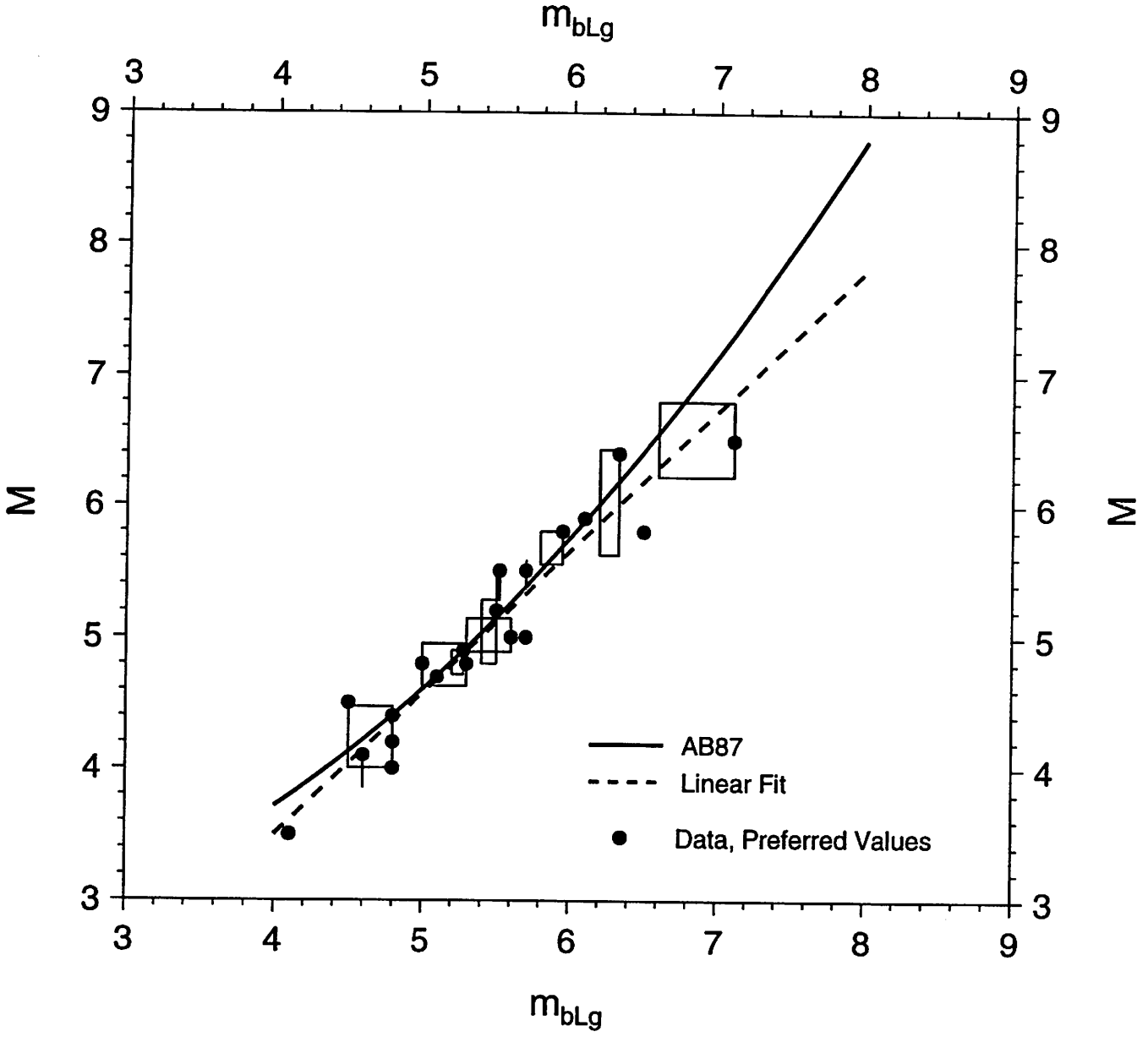

Figure 2. M versus m_{bLg}, revised from Boore and Atkinson (1987). The curve labeled "AB87" is from Atkinson and Boore (1987). Note that although M is the more fundamental source parameter, the short-period magnitude m_{bLg} is used for the abscissa because in most applications in central and eastern North America, the design earthquake will be in terms of m_{bLg}, and a moment magnitude M must be derived from this in order to make ground-motion estimates using seismological models.

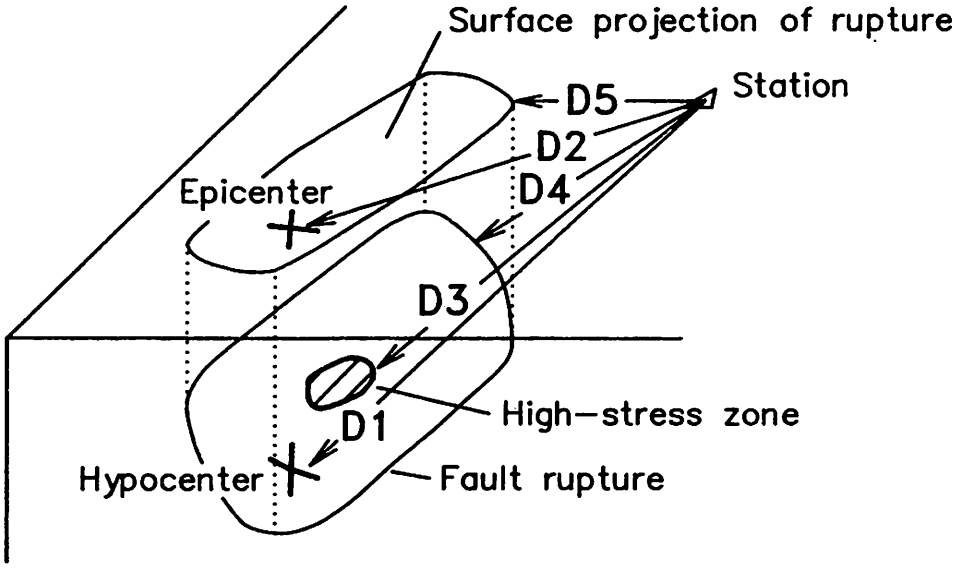

Distance Measures (from recording station)

D1 – Hypocentral

D2 – Epicentral

D3 – Closest distance to high–stress zone

D4 – Closest distance to fault rupture

D5 – Closest distance to surface projection of rupture

Figure 3. Diagram illustrating different distance measures used in relationships for estimating ground motion. (Modified from Shakal and Bernreuter, 1981.)

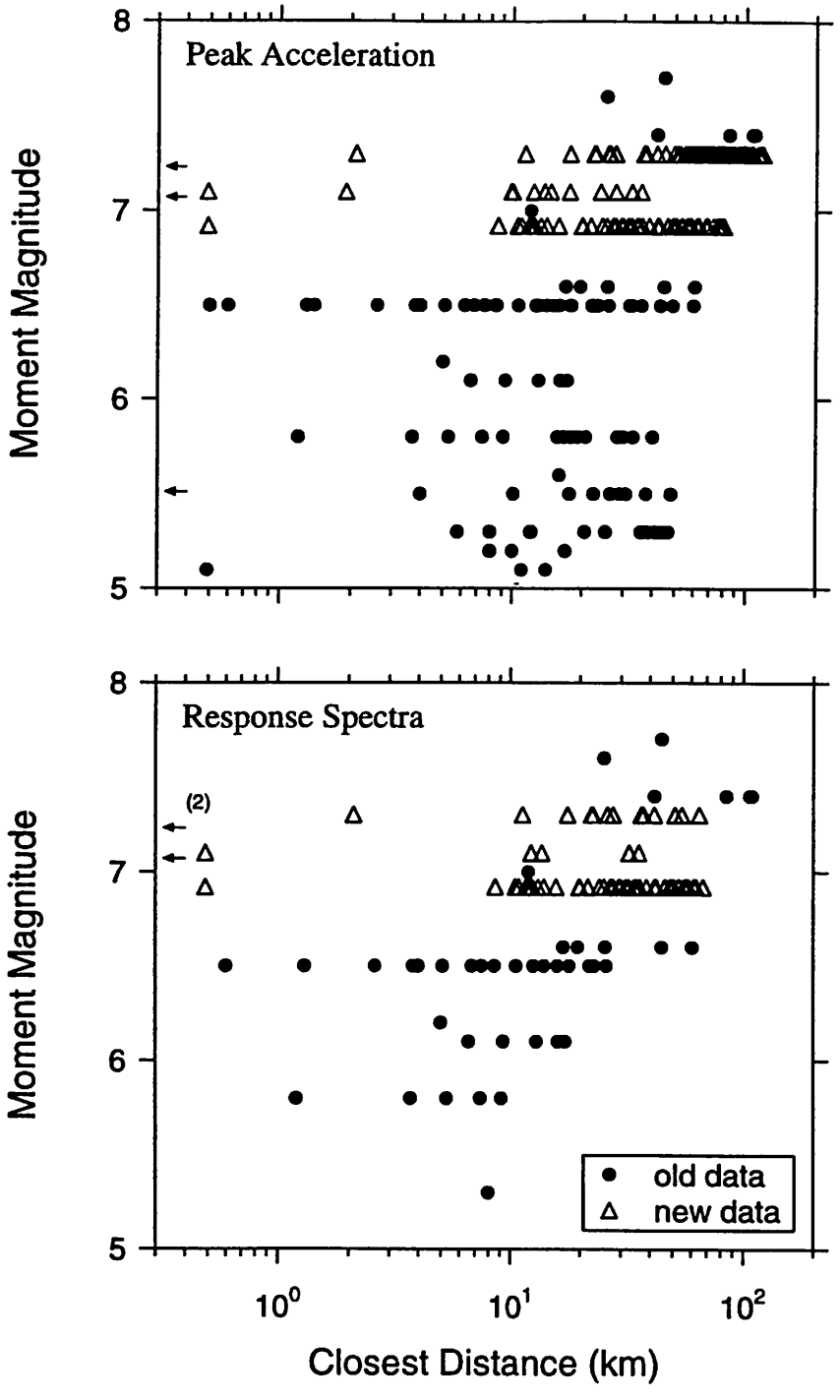

Figure 4. The distribution of the western North America data in magnitude and distance space (each point represents a recording). The data points labeled "old data" were used in previous studies (Joyner and Boore, 1981, 1982); the "new data" were added in the recent work of Boore *et al.* (1993). The points in the top and bottom frames were used in developing equations for peak acceleration and response spectra, respectively. (From Boore *et al.*, 1993.)

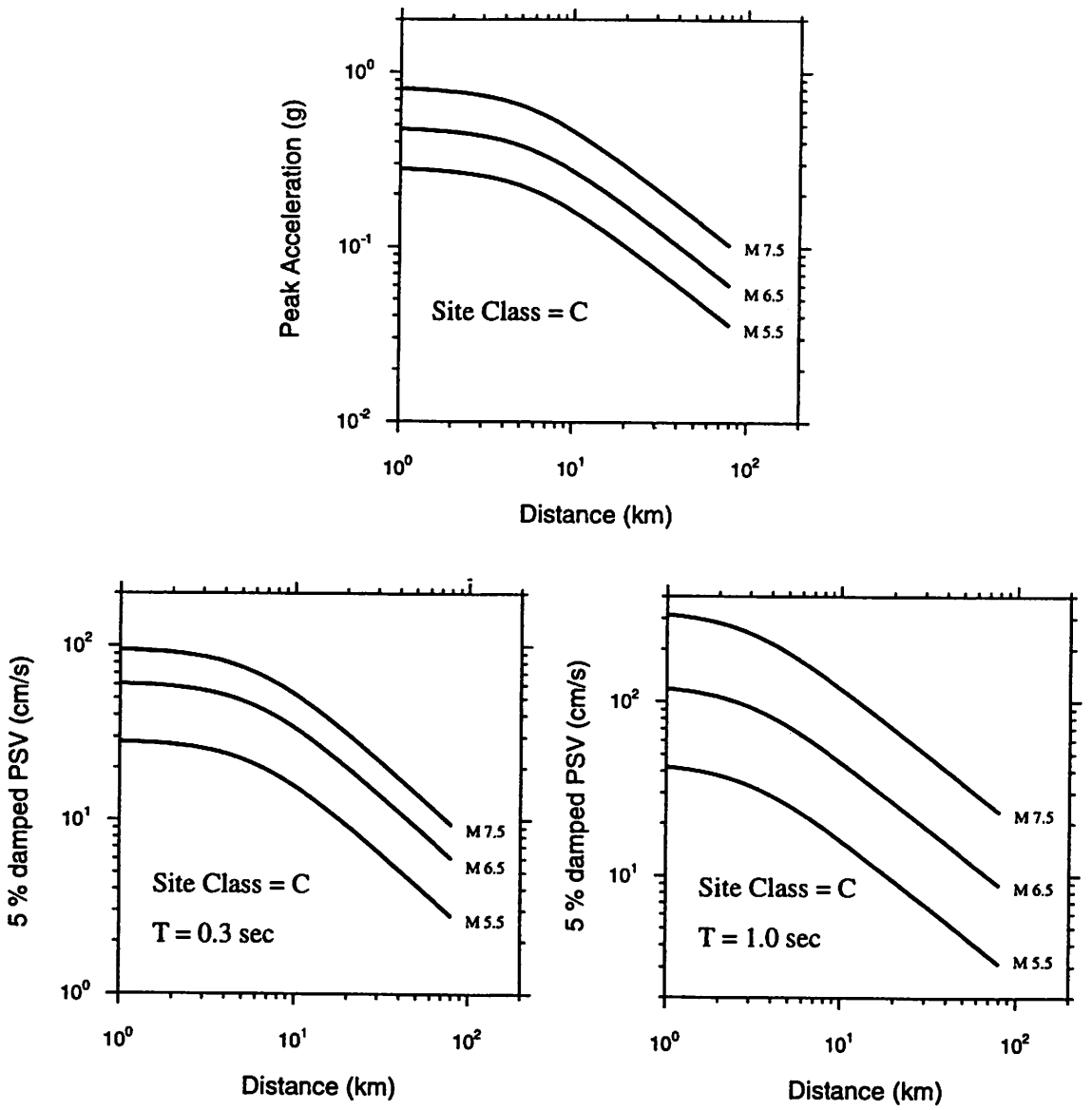

Figure 5. Attenuation with distance of peak acceleration and response spectra for the random horizontal component. (from Boore *et al.*, 1993).

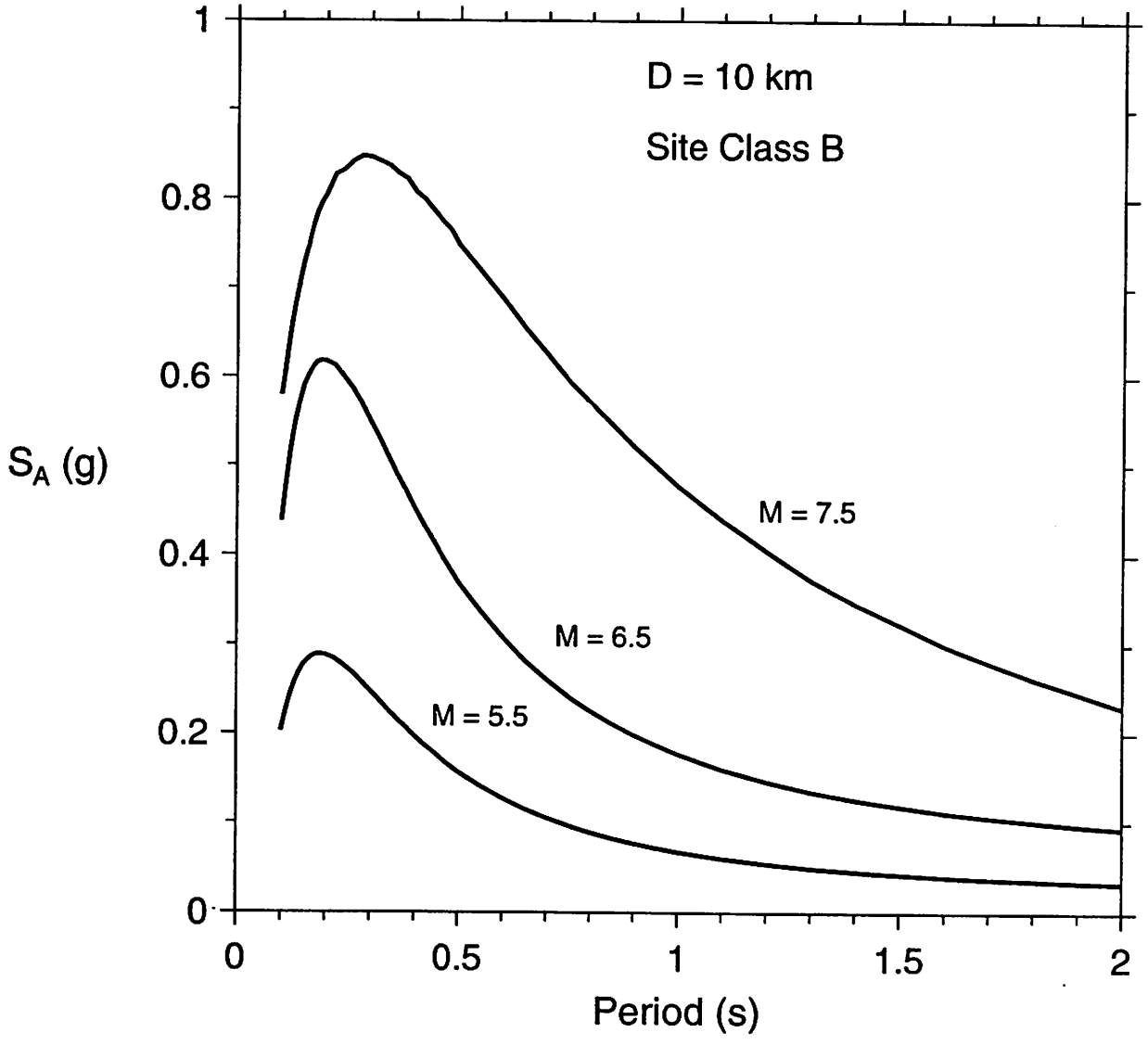

Figure 6. Five-percent damped pseudoacceleration response spectra for a randomly-chosen component of horizontal motion at 10 km for site class *B* and a suite of magnitudes, using the equations of Boore *et al.* (1993).

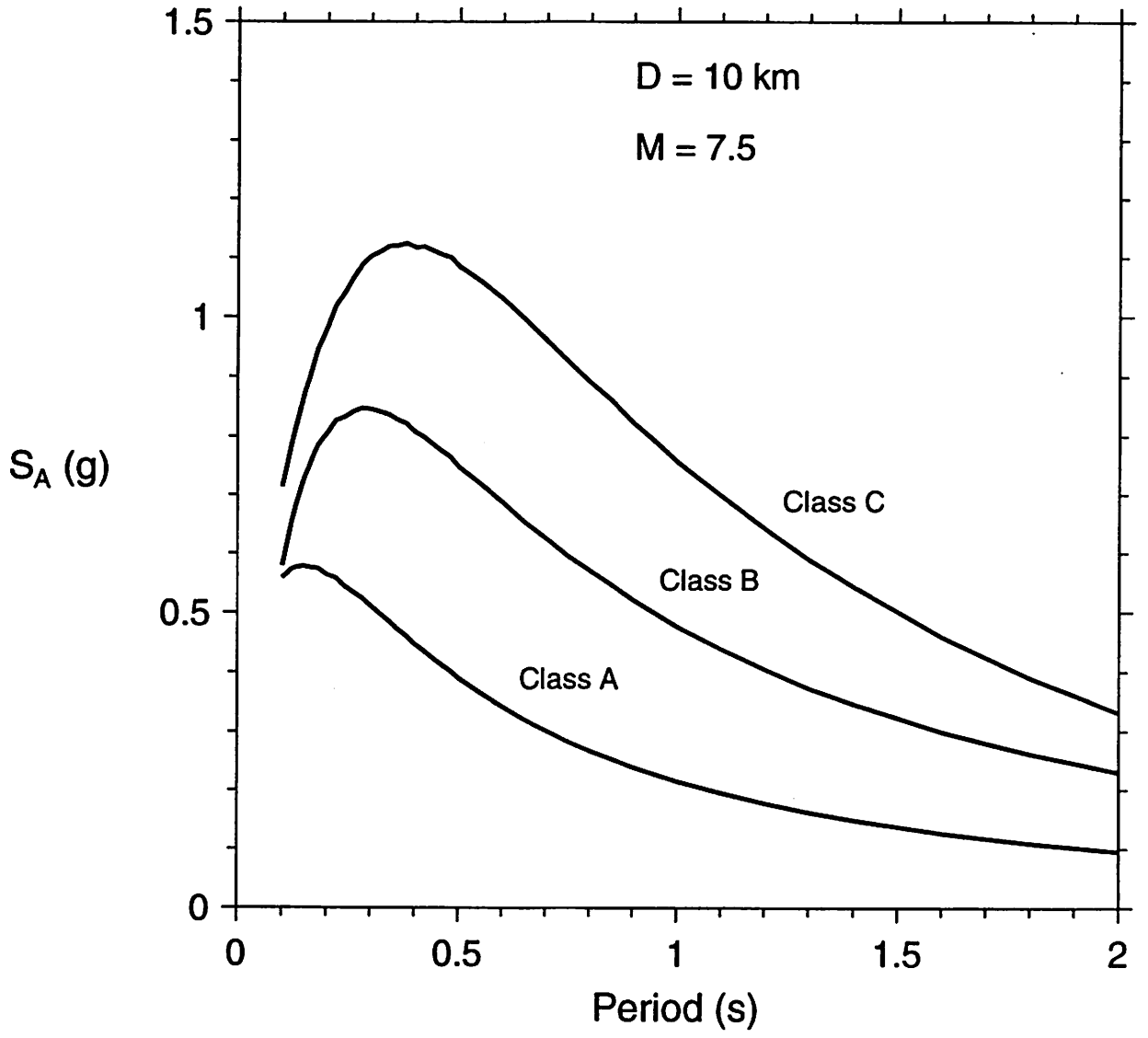

Figure 7. Five-percent damped pseudoacceleration response spectra for a randomly-chosen component of horizontal motion at 10 km for magnitude 7.5 and a suite of site classes, using the equations of Boore *et al.* (1993).

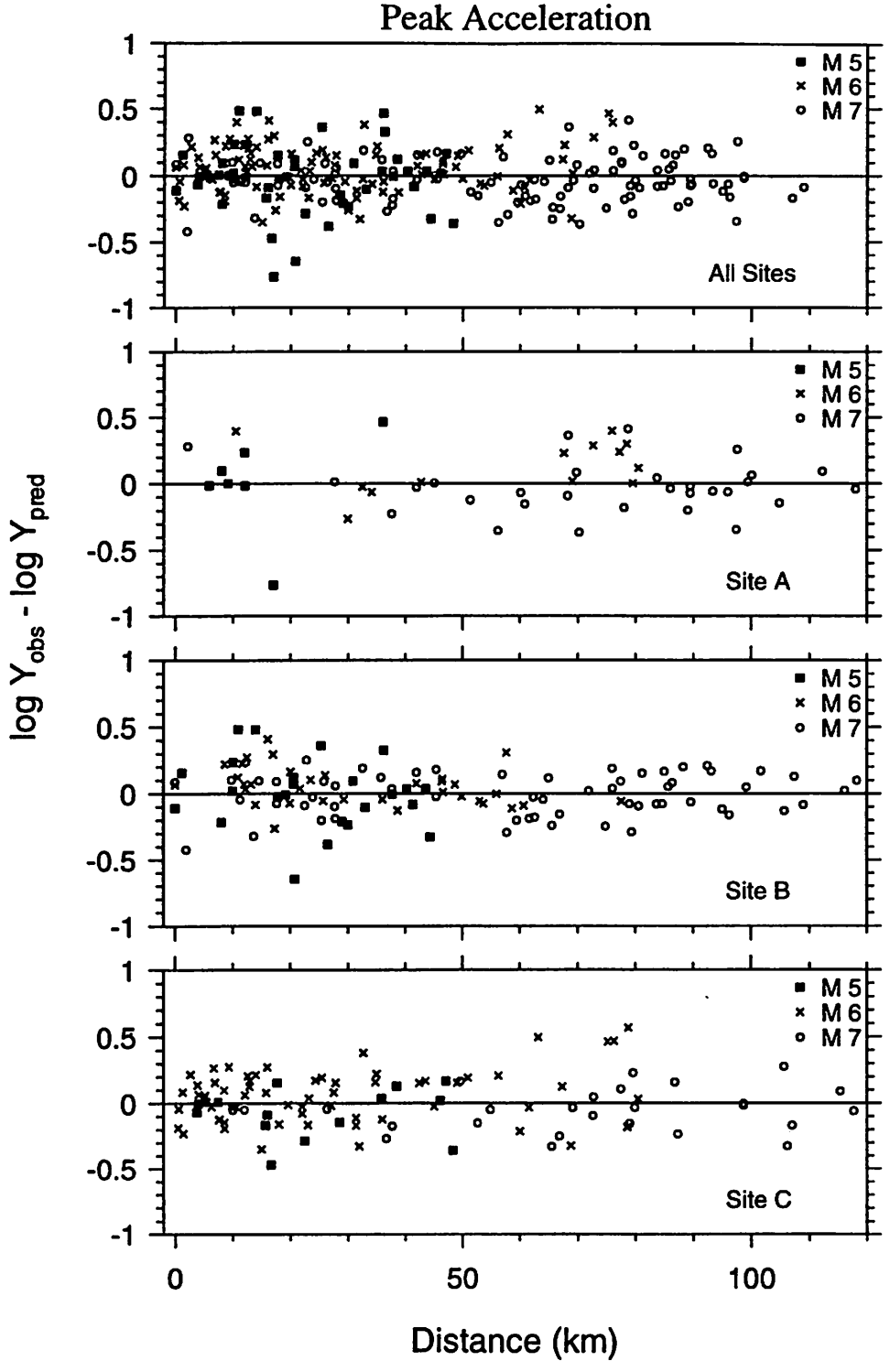

Figure 8. Residuals of peak acceleration ($\log Y_{observed} - \log Y_{predicted}$), as a function of distance for magnitude groups and site classes. (From Boore *et al.*, 1994.)

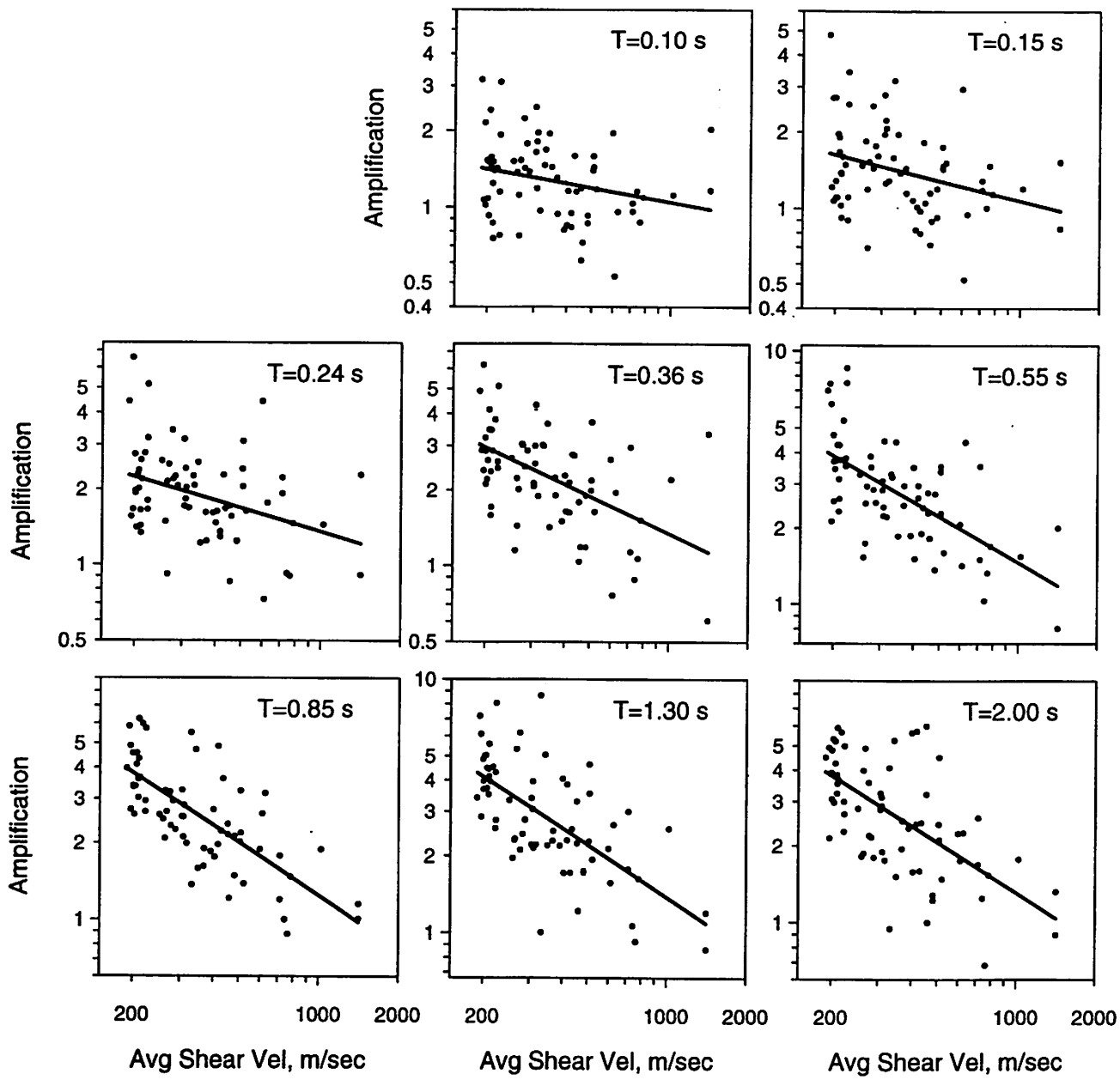

Figure 9. Amplification as a function of average shear velocity, as given by equation (2). The dots are the data used to determine the velocity dependence. (From Boore *et al.*, 1994.)

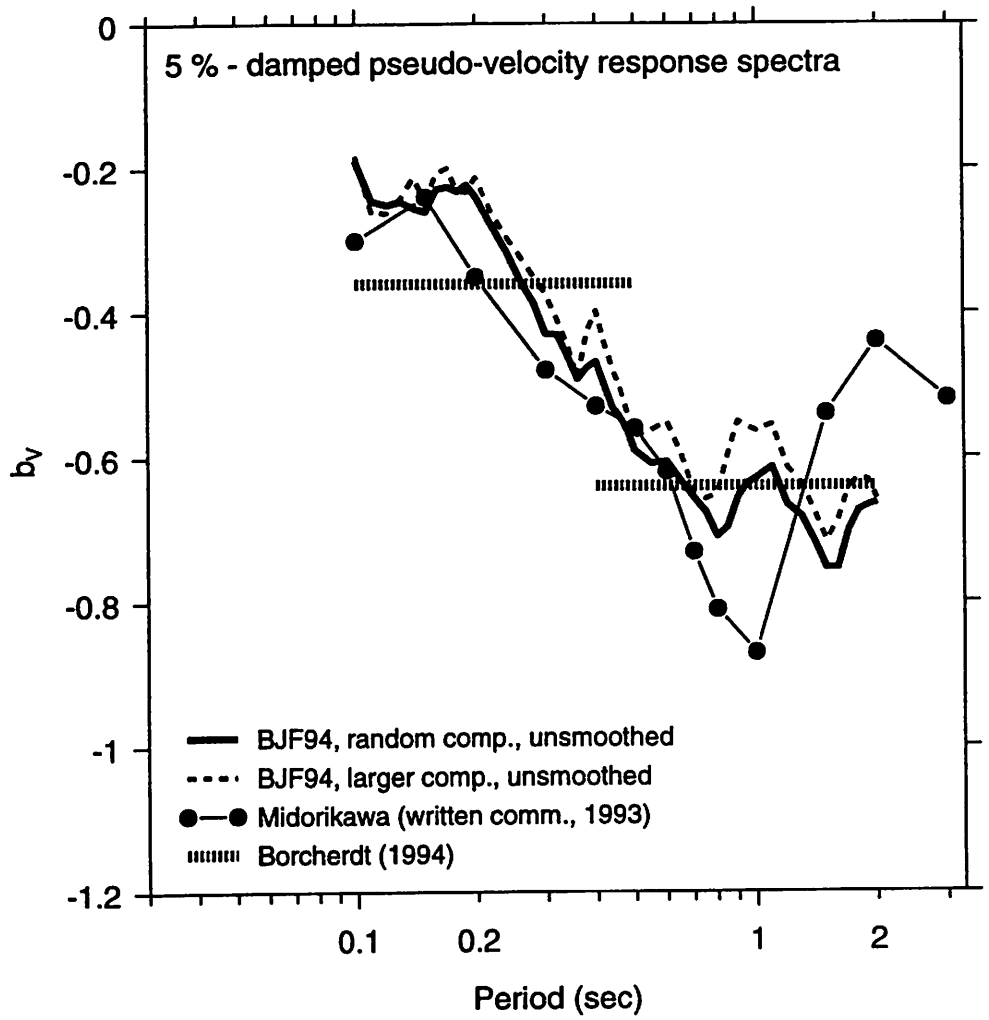

Figure 10. The coefficient that controls the shear-velocity dependence of response spectral amplification, as determined by Boore *et al.* (1994) for California data and by Midorikawa (written communication, 1993) for data from Japan. Also shown are the coefficients proposed by Borcherdt (1994) for determining short-period and mid-period amplification factors in building codes; these were determined from Fourier amplitude spectra of recordings from the Loma Prieta earthquake.

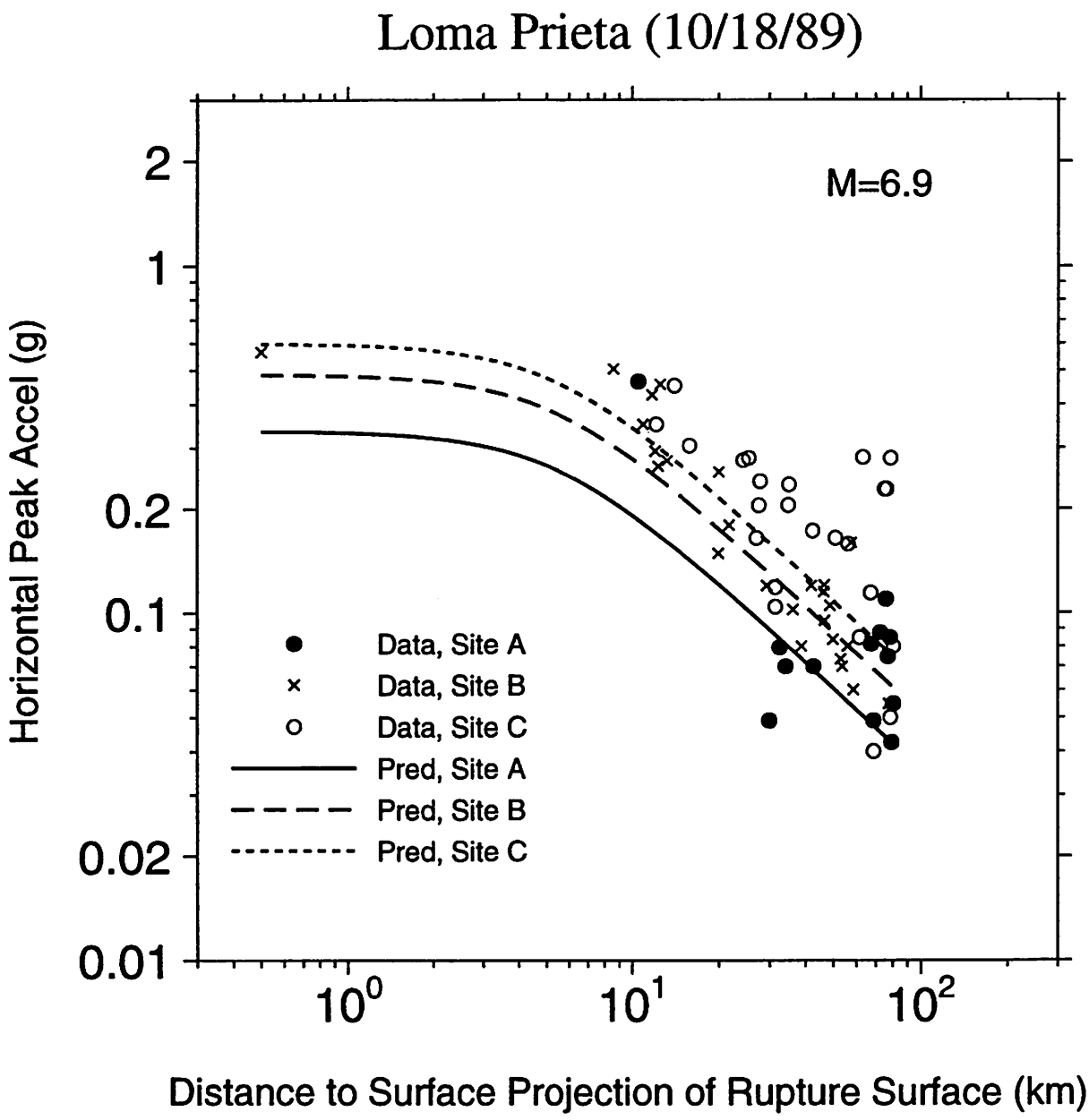

Figure 11. Peak horizontal acceleration as a function of distance for the 1989 Loma Prieta earthquake, compared with predictions from Boore *et al.* (1993).

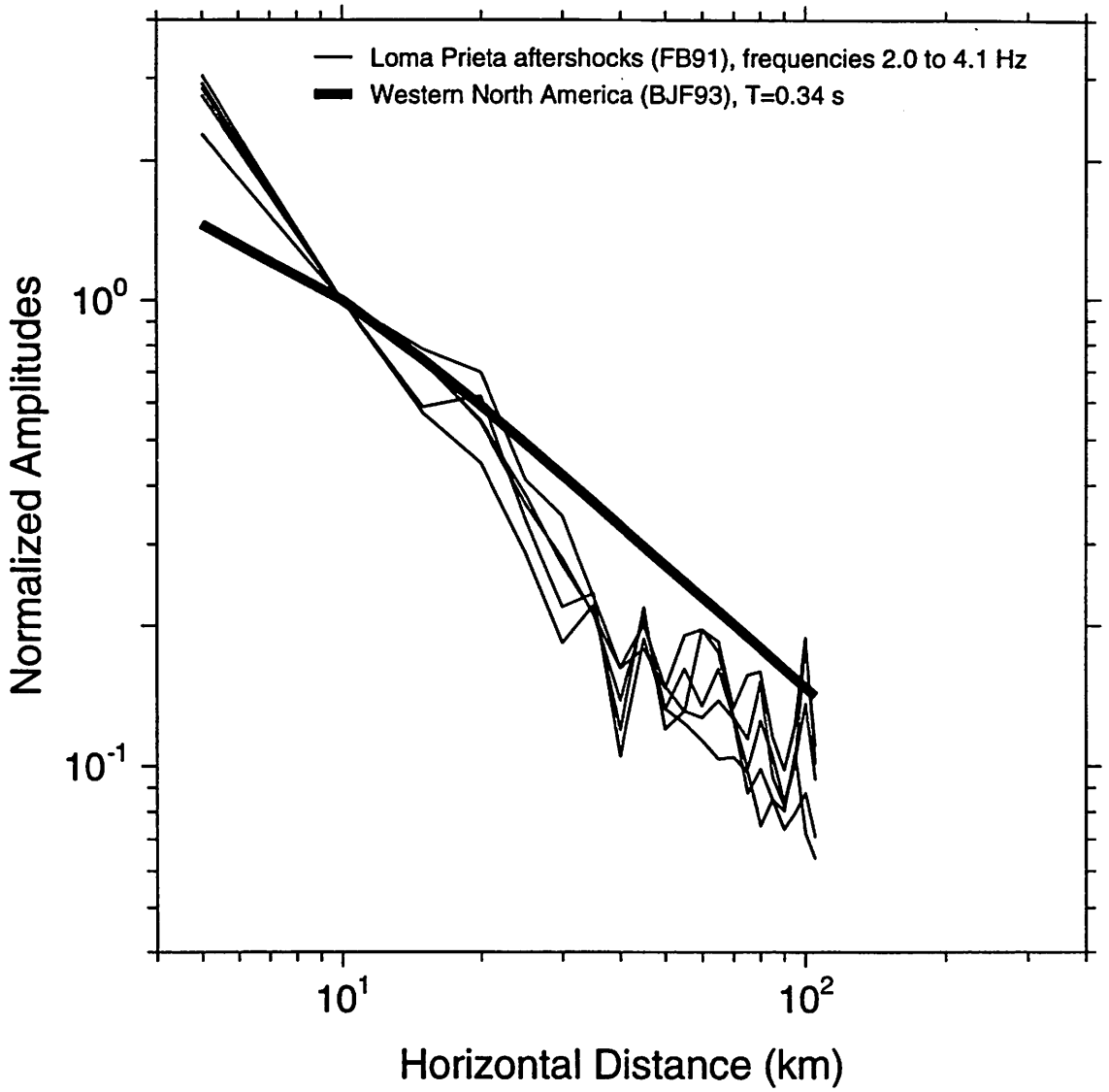

Figure 12. Decay of Fourier spectral amplitudes for aftershocks recorded along a line from the Loma Prieta source region to San Francisco (Fletcher and Boatwright, 1991), compared to the attenuation of response spectra determined by Boore *et al.* (1993) at a period consistent with the frequencies of the Fourier spectral components. The relative placement of the response spectral and Fourier amplitude data on the ordinate is arbitrary; only the relative change in amplitude with distance is important. We have normalized the curves to unity at 10 km.

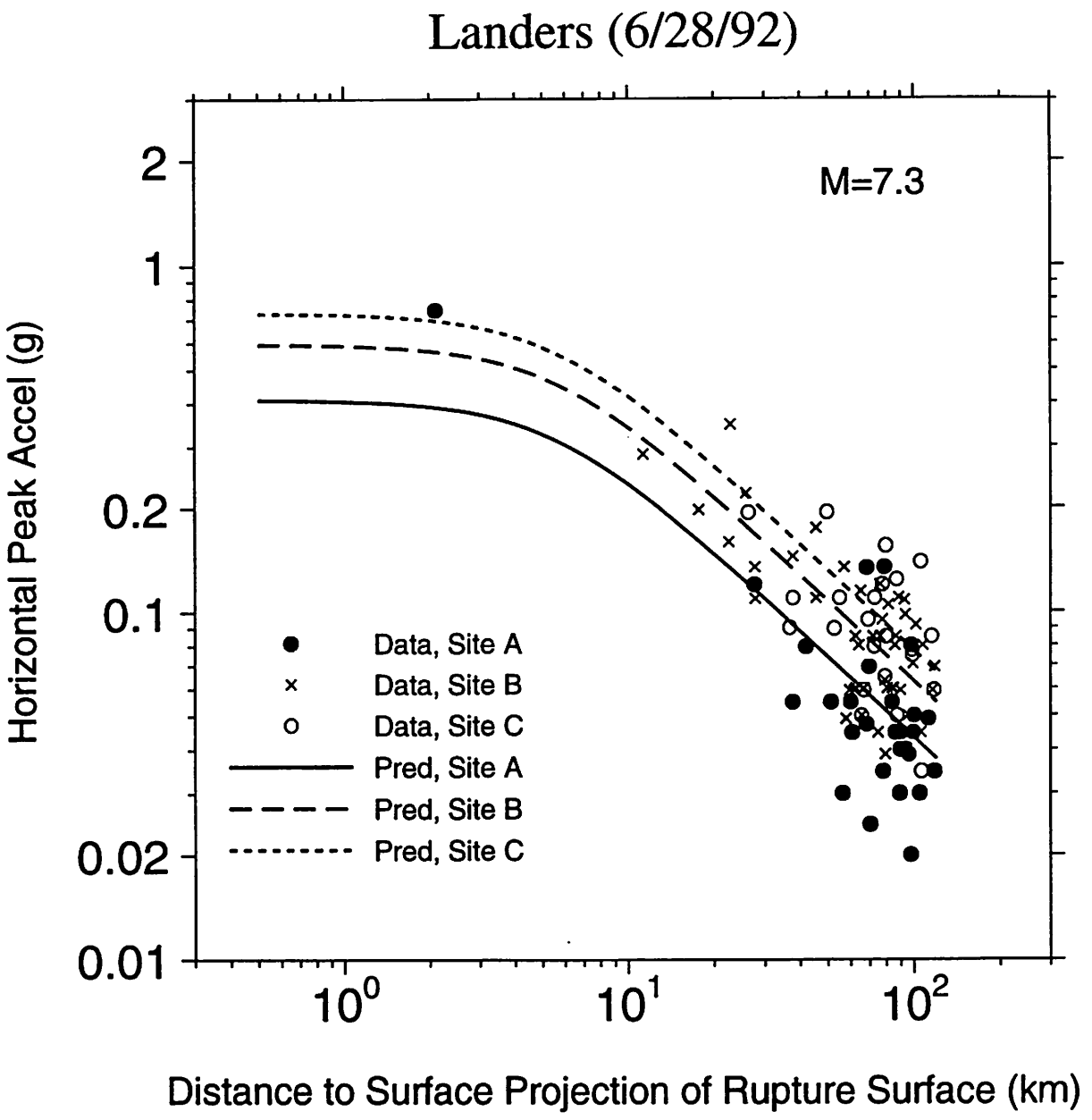

Figure 13. Peak horizontal acceleration as a function of distance for the 1992 Landers earthquake, compared with predictions from Boore *et al.* (1993).

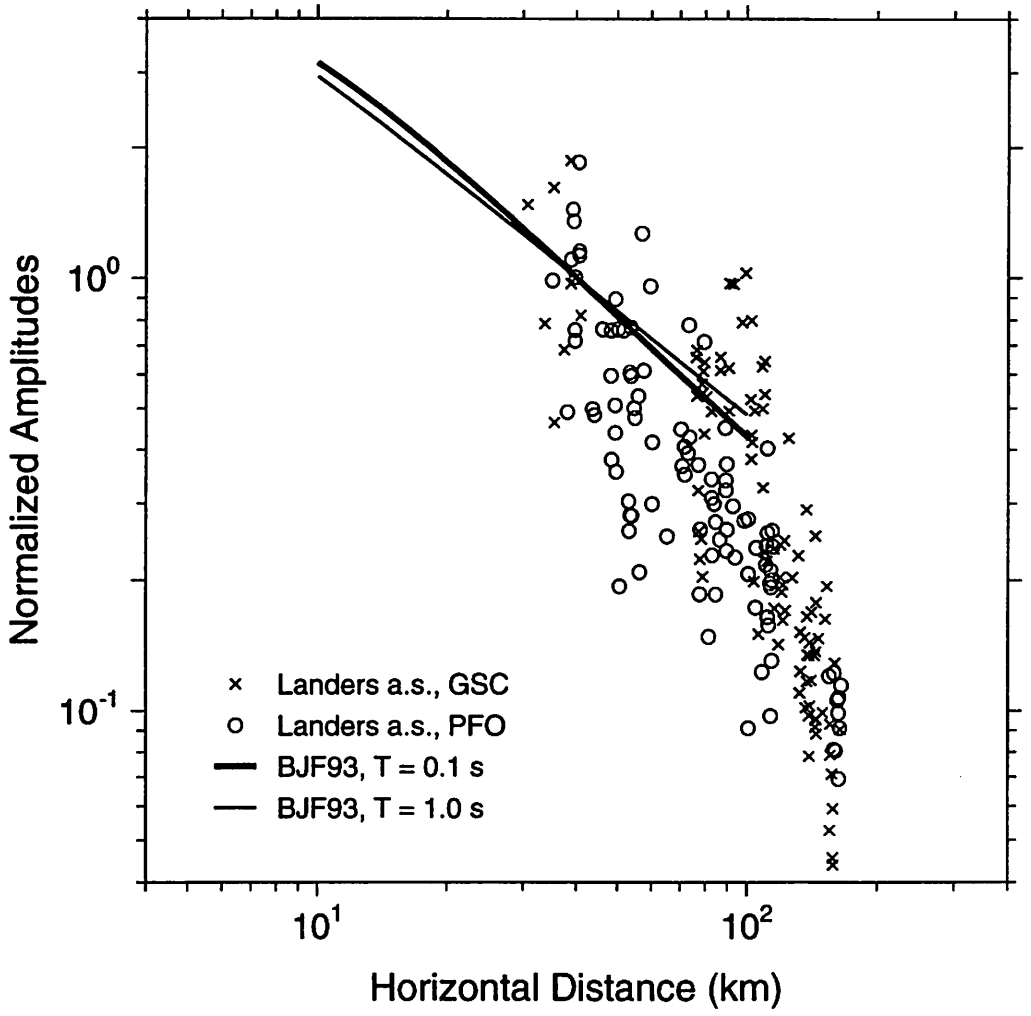

Figure 14. Decay of amplitudes for Landers aftershocks recorded at GSC and at PFO (from Mori, 1993), compared to the attenuation of response spectra determined by Boore *et al.* (1993) at periods consistent with the frequencies of the aftershock recordings. The aftershocks of the Landers earthquake are distributed along a more-or-less linear trend extending for more than 80 km, with stations GSC and PFO to the north and south of the aftershock zone, respectively. Mori (1993) took advantage of the source and station distributions to construct profiles in which the source location changed and the recorder location was fixed, the inverse of the usual situation. This eliminates variations in site response, but requires a normalization for the varying magnitudes of the aftershocks. Mori (1993) normalized the motions to a common magnitude. The relative placement of the response-spectral predictions and the aftershock data on the ordinate is arbitrary; only the relative change in amplitude with distance is important. We have normalized the curves and an approximate average of the aftershock data to unity at 40 km. Note the very different amplitude dependence for paths to GSC and to PFO (the azimuths of the paths from the source regions to these stations differ by approximately 180 degrees).

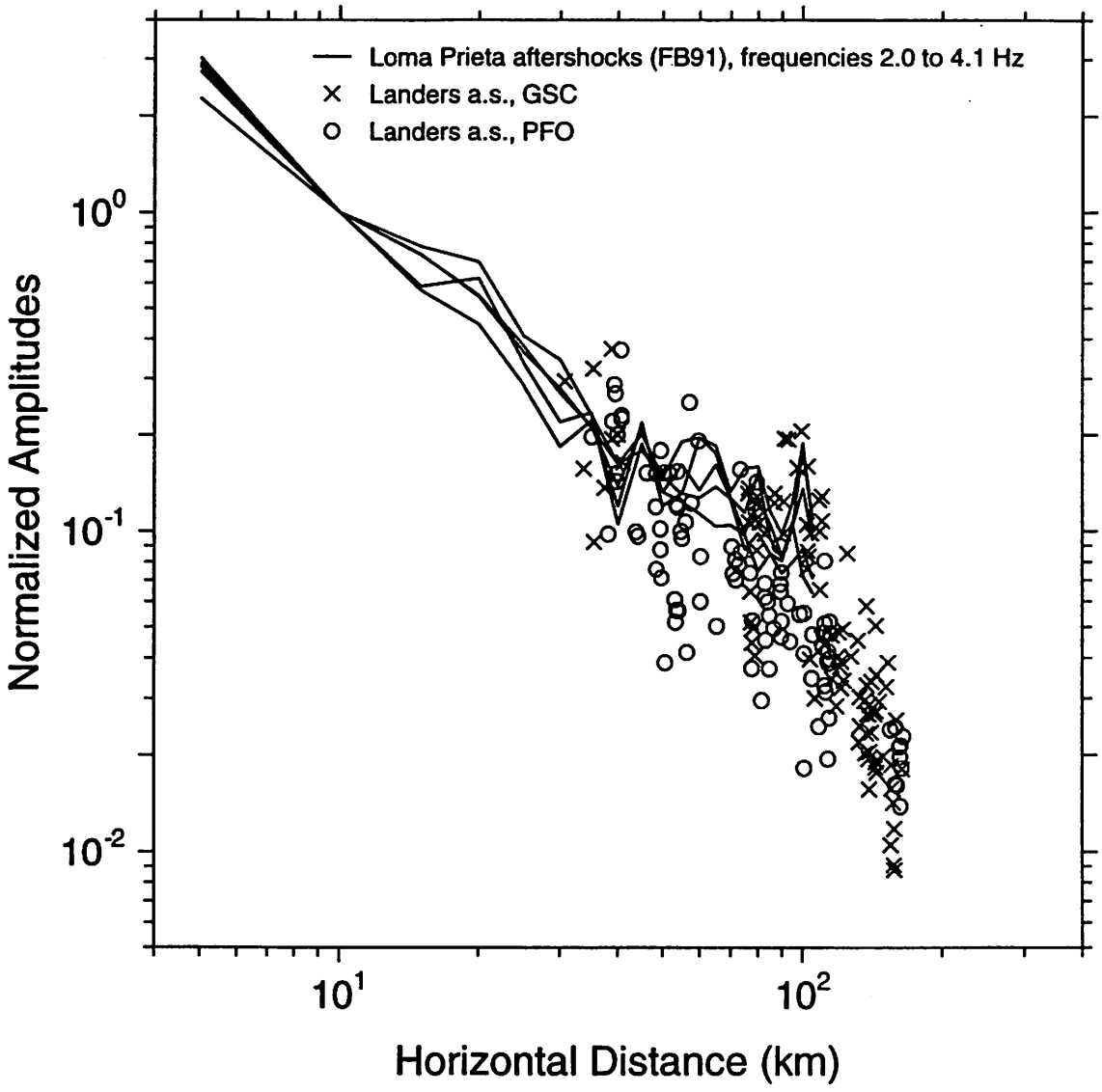

Figure 15. The aftershock attenuation from Loma Prieta and Landers shown in Figures 13 and 14, combined into one figure by applying an adjustment factor to the Landers data such that it approximately agrees with the Loma Prieta results near 40 km.

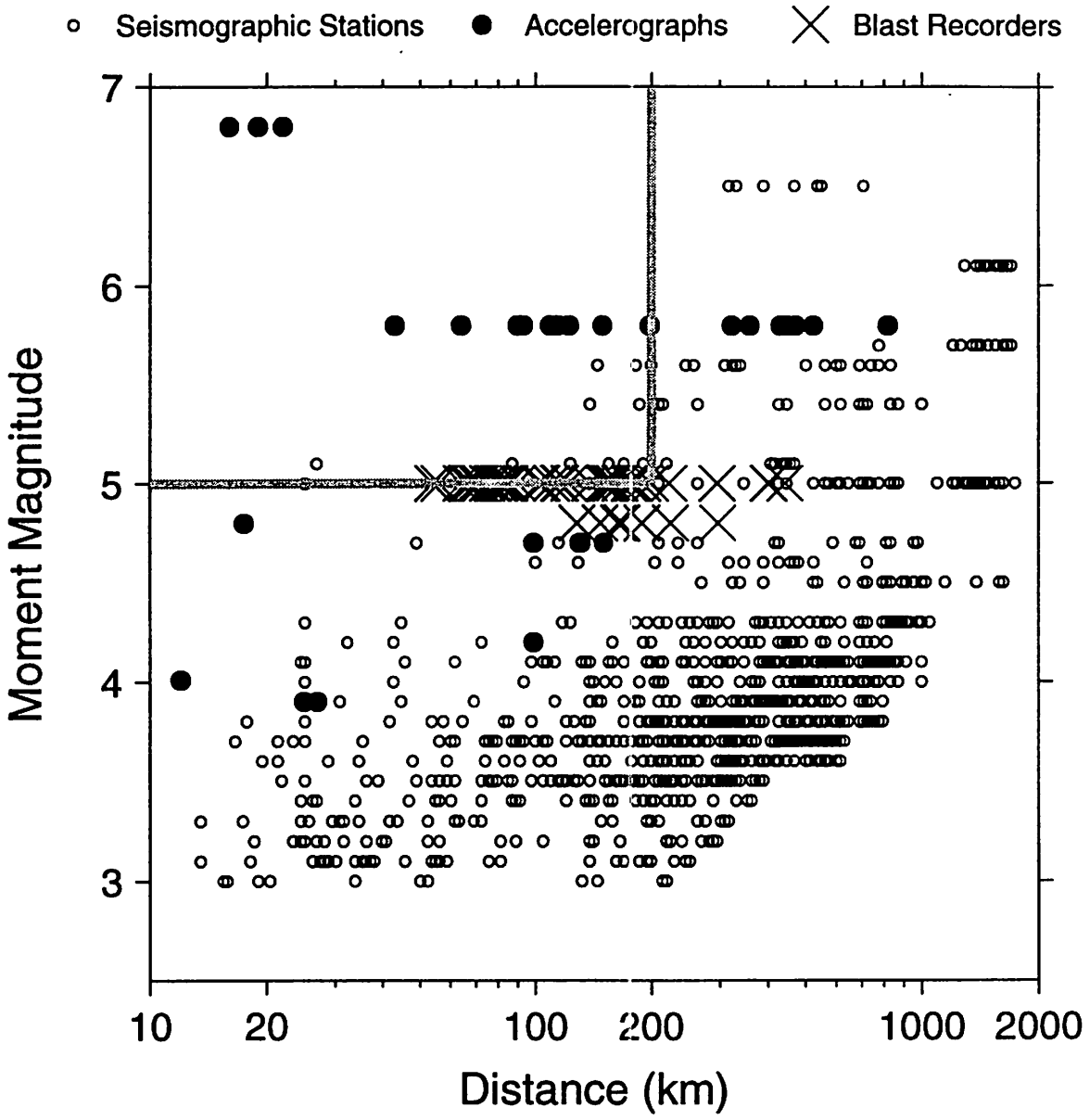

Figure 16. Distribution in magnitude and distance of ground-motion recordings in central and eastern North America. Three symbols have been used to indicate whether the recording was from an accelerograph (primarily SMA-1 analog recorders), a standard seismological station, whose output is proportional to velocity for most frequencies (most of these data are from the ECTN, as provided by G. Atkinson), or a blast recorder (Street *et al.*, 1987; Street *et al.*, 1988). The shaded line outlines the boundaries of the plot showing the magnitude and distance distribution for recordings in western North America (Figure 4).

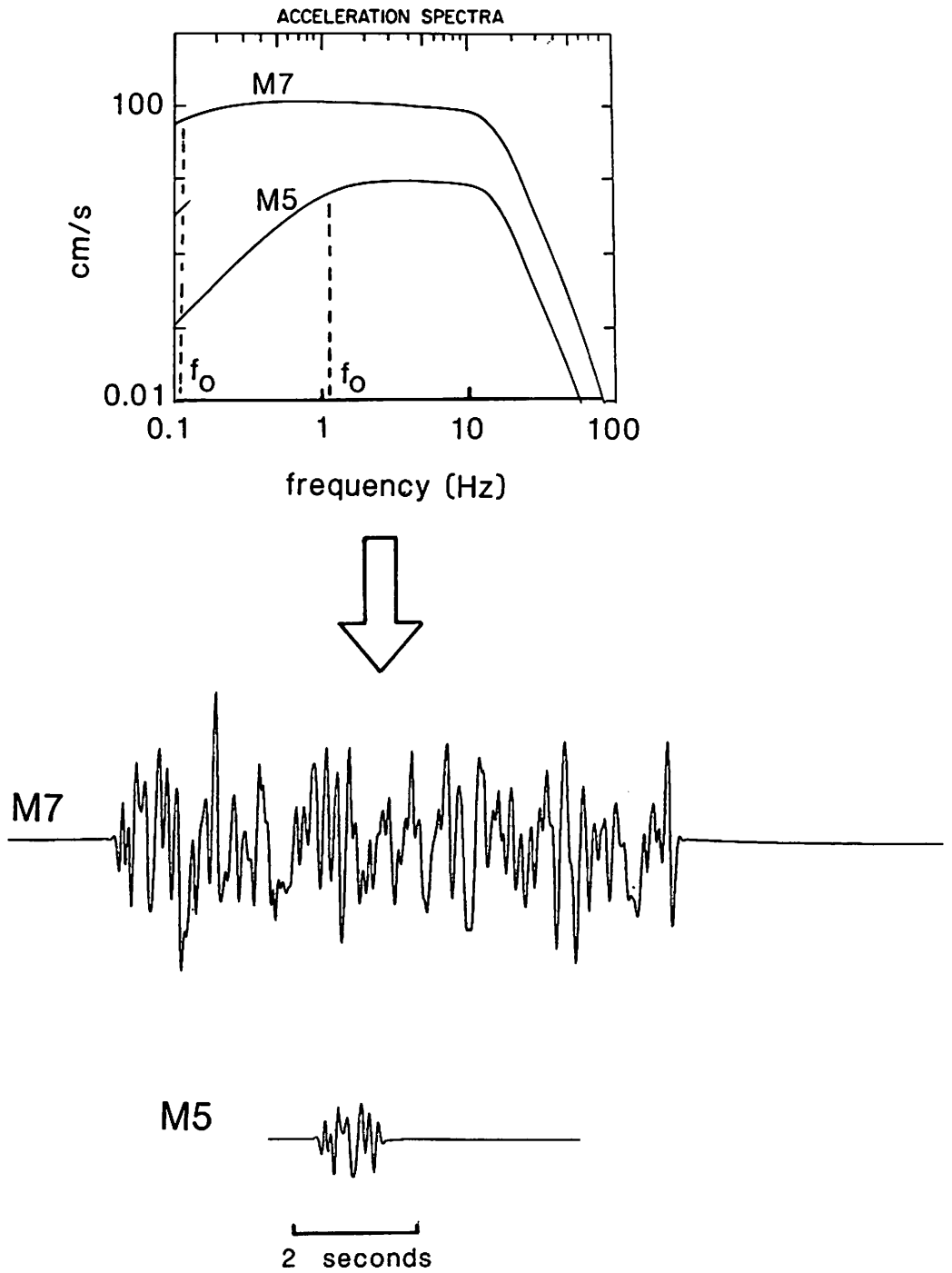

Figure 17. Basis of stochastic model. Radiated energy described by spectra in the upper part of the figure is assumed to be distributed randomly over a duration equal to the inverse of the lower-frequency corner (f_0). The time series in the lower part of the figure are one realization of a random process. The levels of the low-frequency part of the spectra are directly proportional to seismic moment. The curves and time series shown are from an actual simulation and indicate the difference in amplitude and duration expected for these two magnitudes. (From Boore, 1989.)

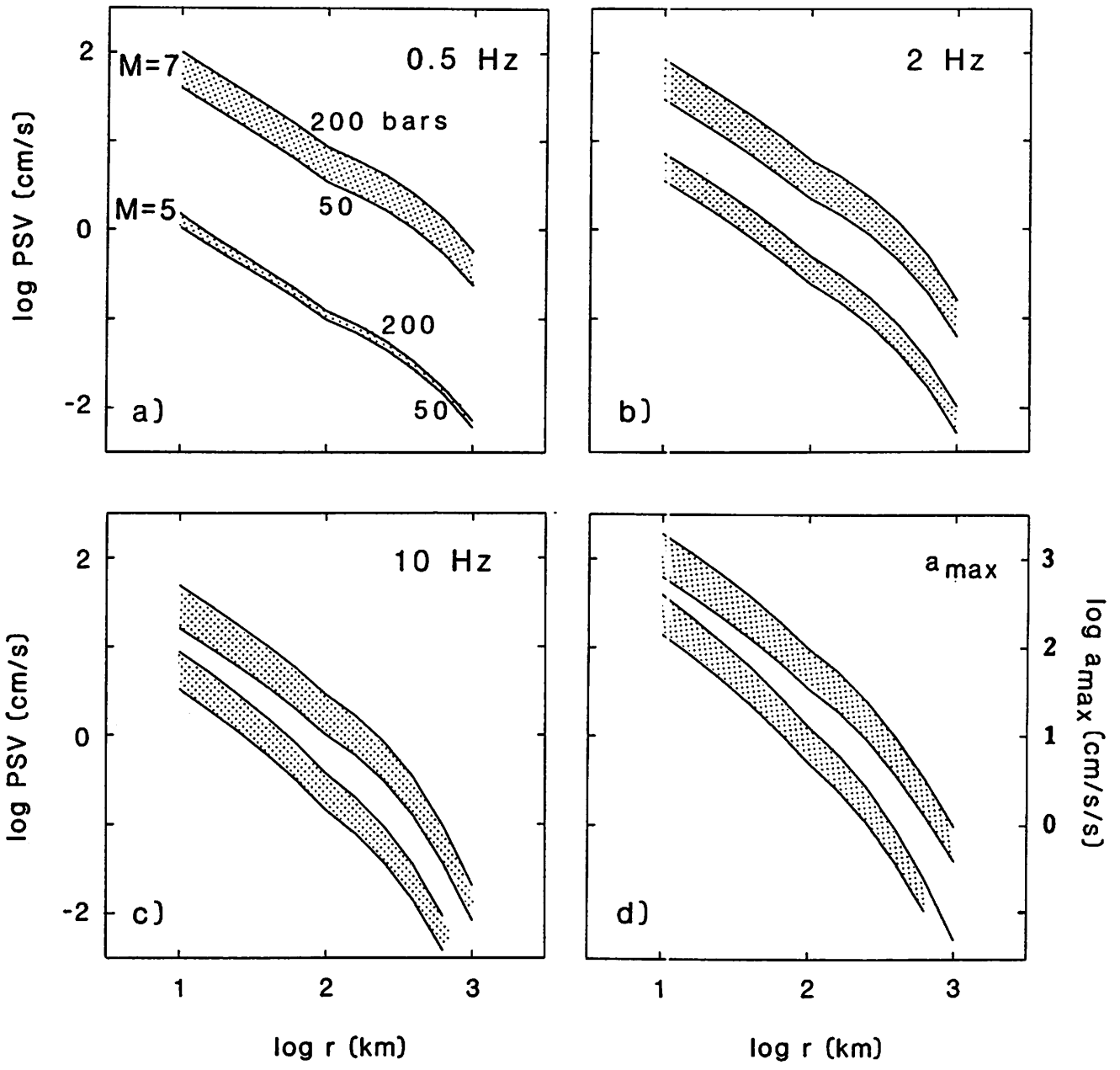

Figure 18. Ground motions for a range of stress parameters. (From Boore and Atkinson, 1987.)

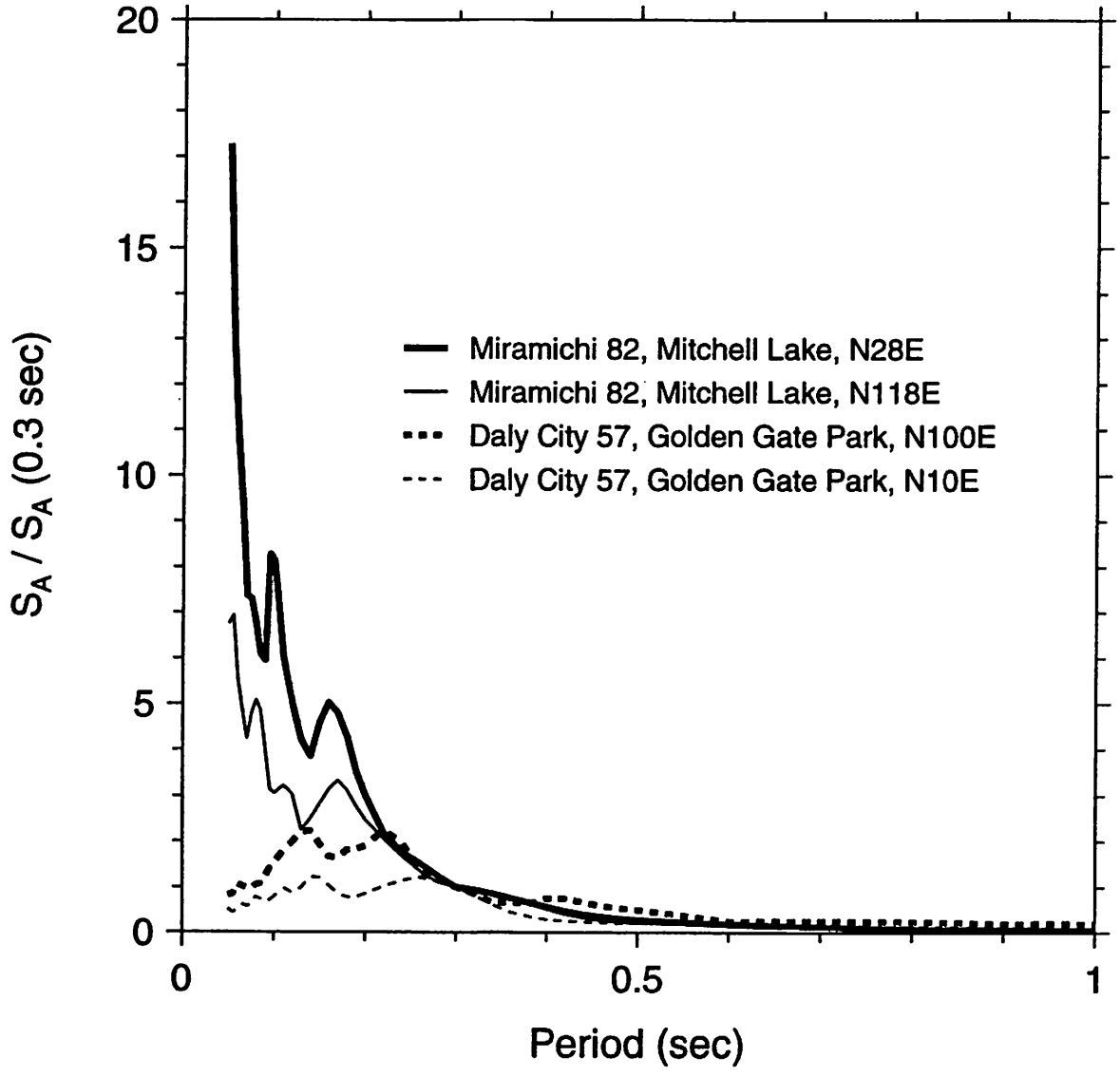

Figure 19. Acceleration response spectra, normalized to the value at 0.3 sec, for rock recordings of the 1957 Daly City earthquake in California and an aftershock of the 1982 Miramichi, New Brunswick, earthquake.

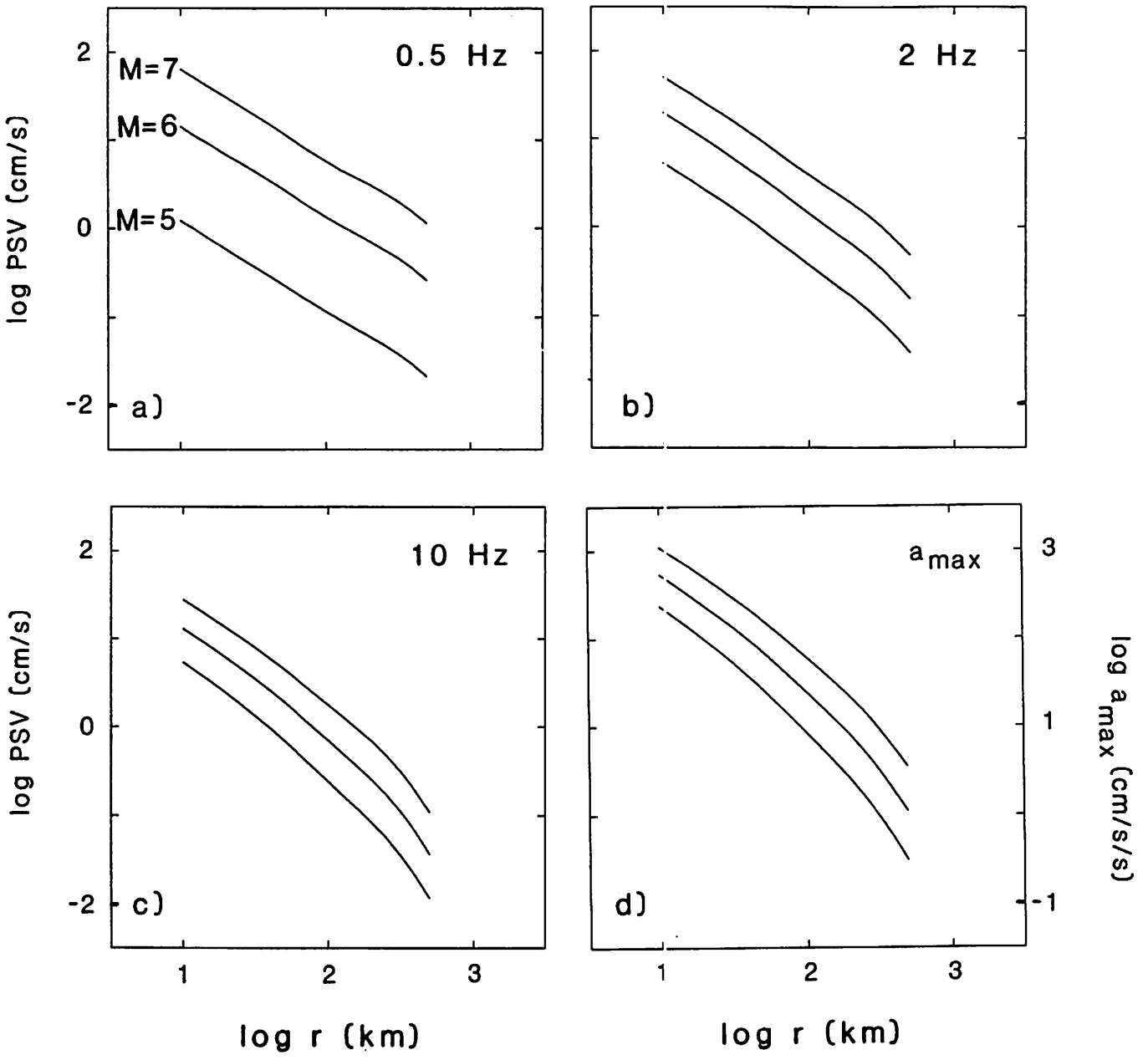

Figure 20. Ground motion at hard-rock sites as a function of distance for a suite of moment magnitudes. (From Boore and Atkinson, 1987.)

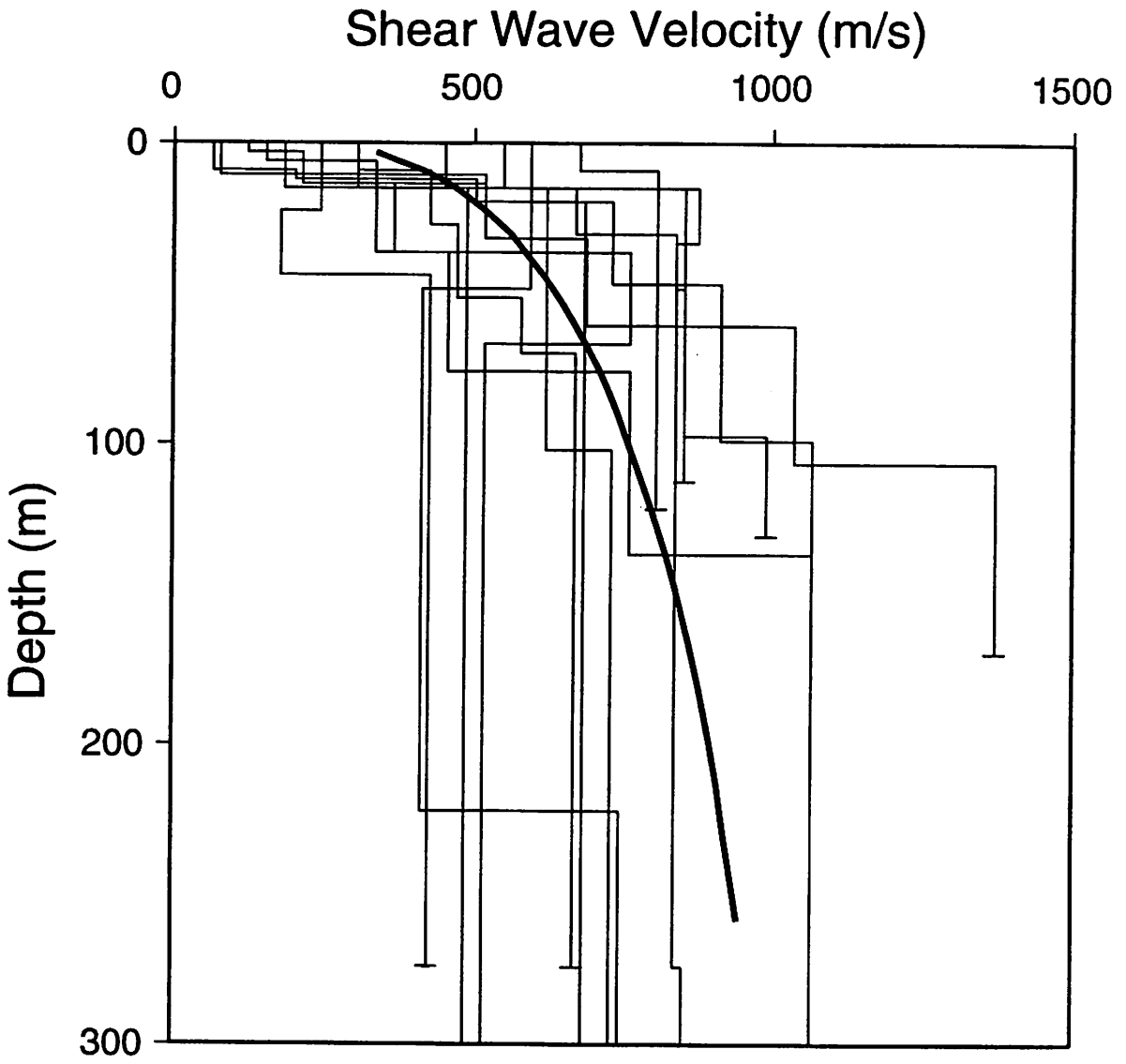

Figure 21. Shear velocity as a function of depth for an average deep-soil site (heavy line), based on a compilation of velocities from PSAR and FSAR reports for nuclear power-plant sites throughout the United States (light lines). The short horizontal bars indicate bedrock. (From Boore and Joyner, 1991, who adapted it from a figure in Bernreuter *et al.*, 1989, who in turn obtained it from W. Silva (personal communication).)

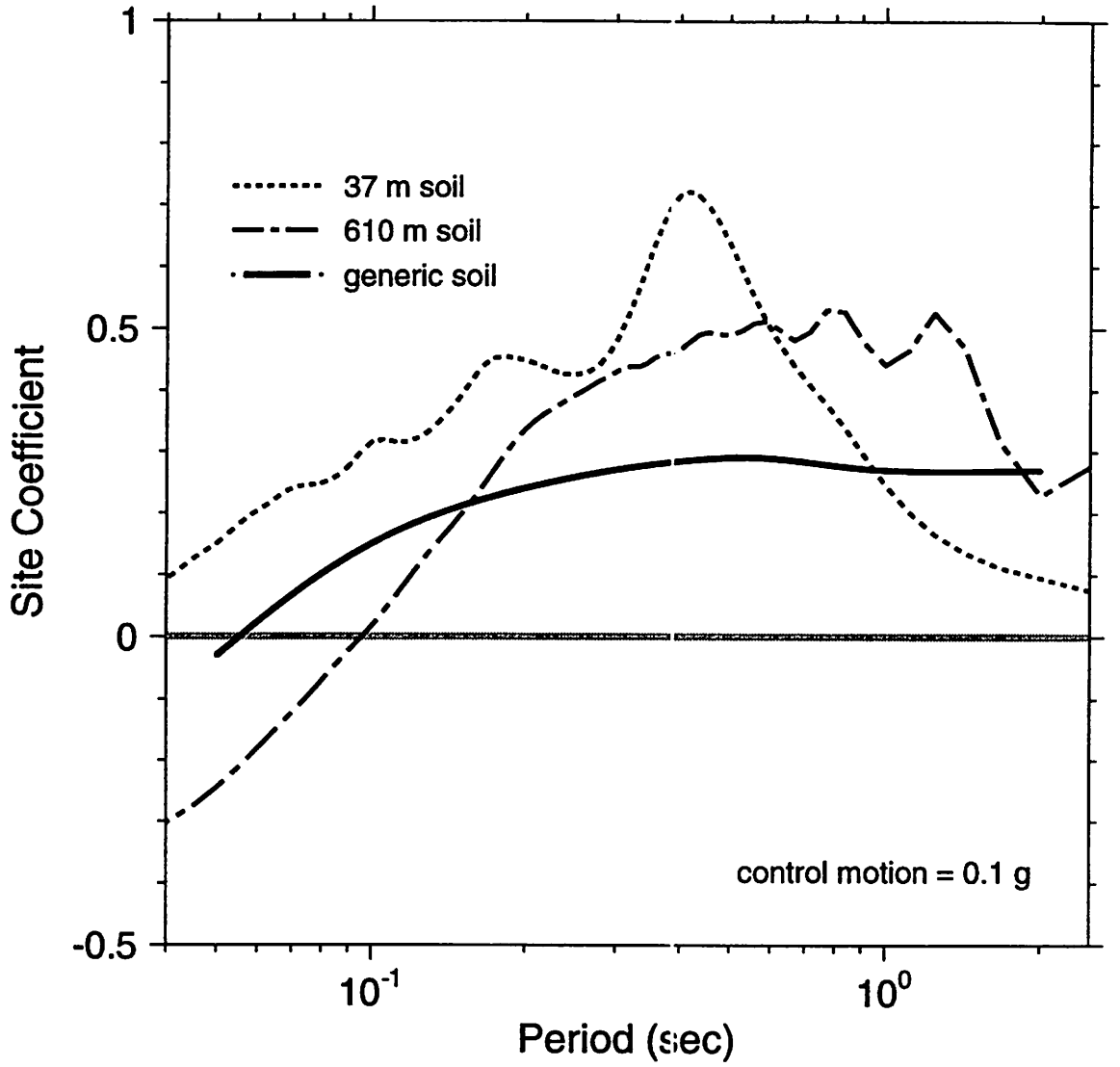

Figure 22. Site coefficients ("*e*" in equation (1)) as a function of oscillator period for a generic firm, deep-soil site (from Boore and Joyner, 1991) and two specific sites in the vicinity of New Madrid, Tennessee (see Toro *et al.*, 1992 for a discussion of the soil profiles; the figure was constructed from data provided by W. Silva).

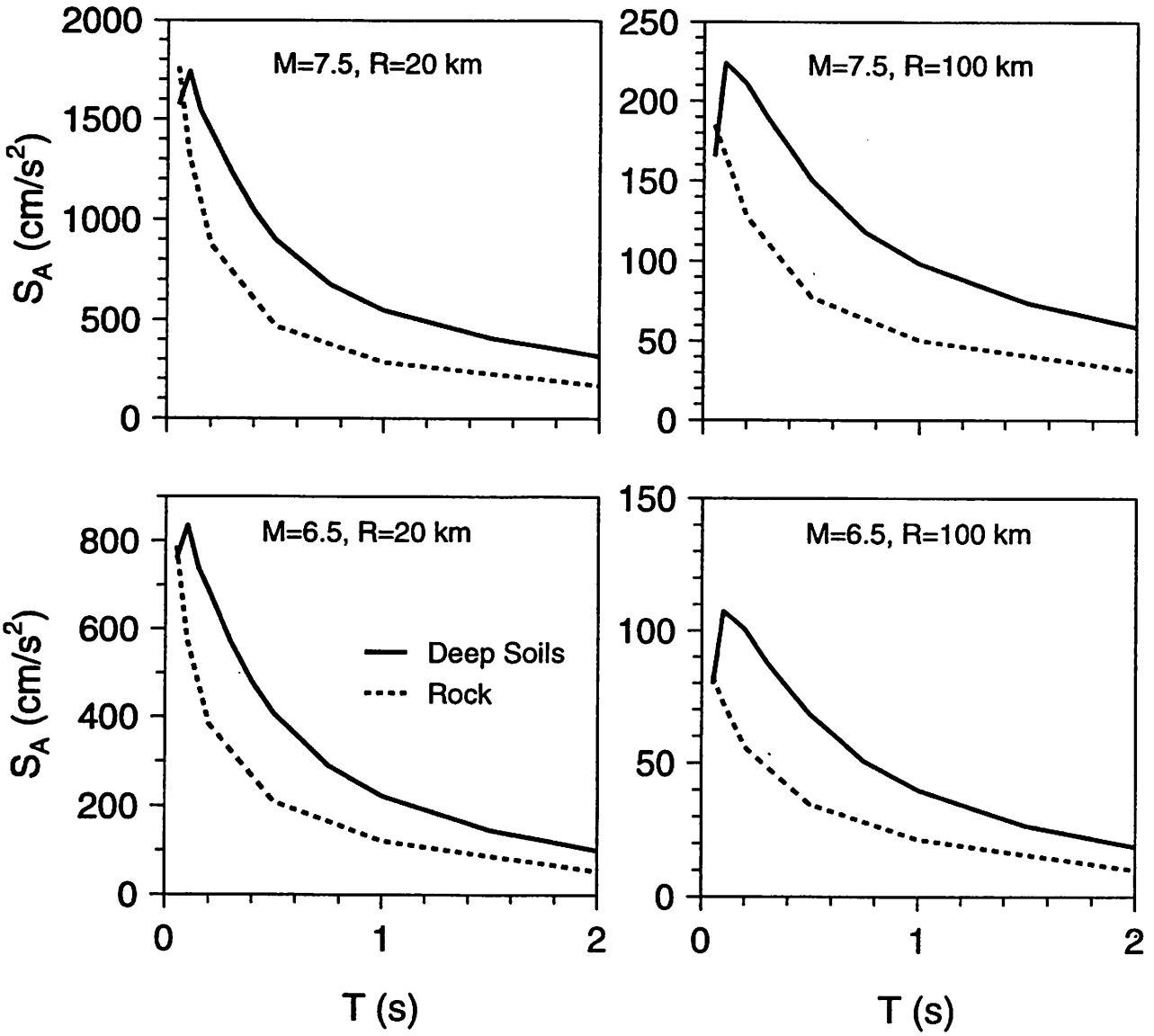

Figure 23. Comparison of pseudoacceleration spectra in central and eastern North America at hard-rock and deep-soil sites, both based on the same methodology. The comparison is for moment magnitudes of 6.5 and 7.5 and hypocentral distances of 20 and 100 km. (From Boore and Joyner, 1991.)

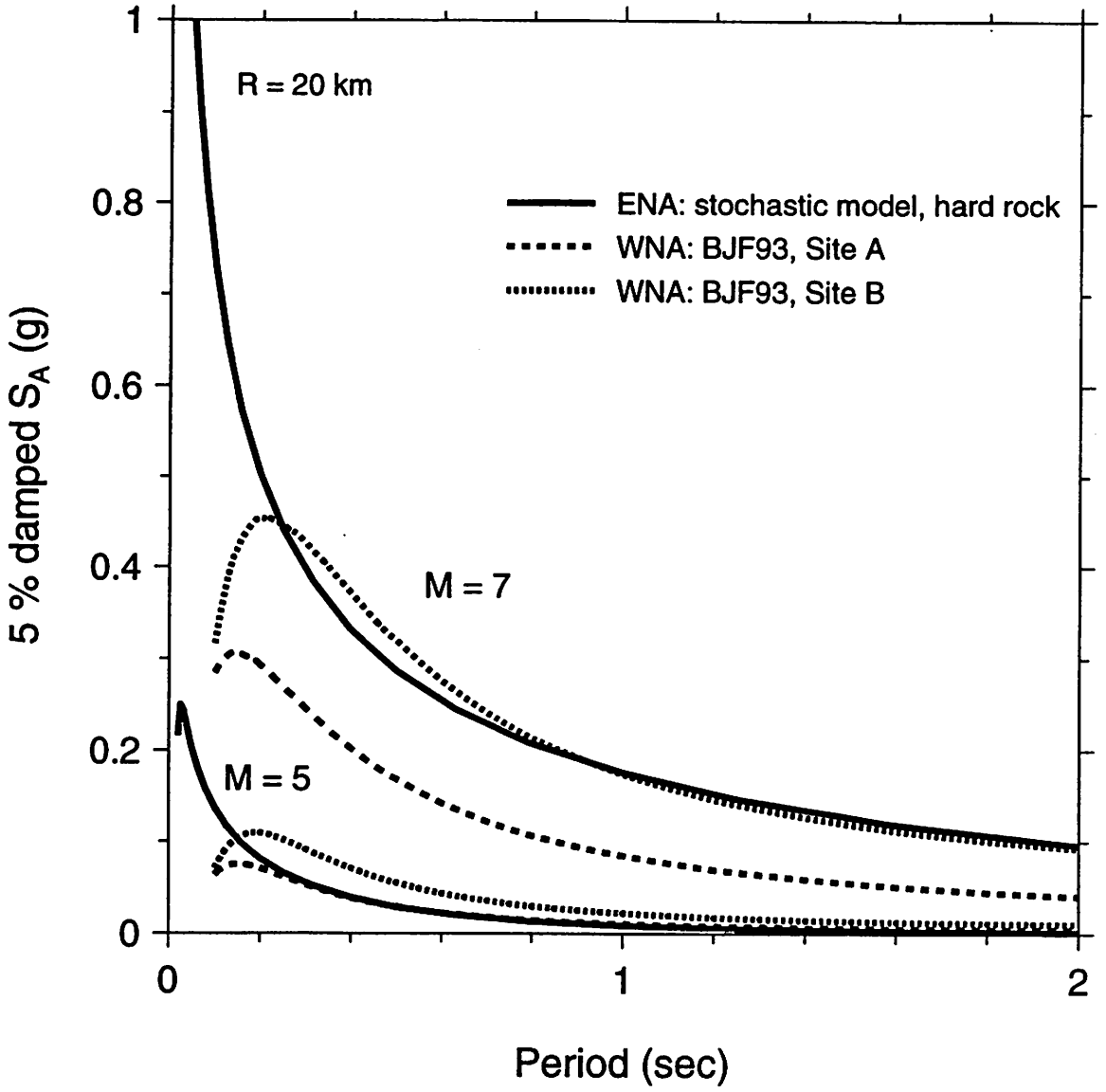

Figure 24. Comparison of acceleration response spectra at rock sites in western North America (WNA) and eastern North America (ENA). The WNA results are from the empirical analysis of Boore *et al.* (1993), and the ENA results are computed using the stochastic model and the parameters of Boore and Atkinson (1987) and Boore and Joyner (1991). The WNA results are given for site classes A and B. Note the large difference in spectral acceleration at short periods, similar to the results in Figure 19.

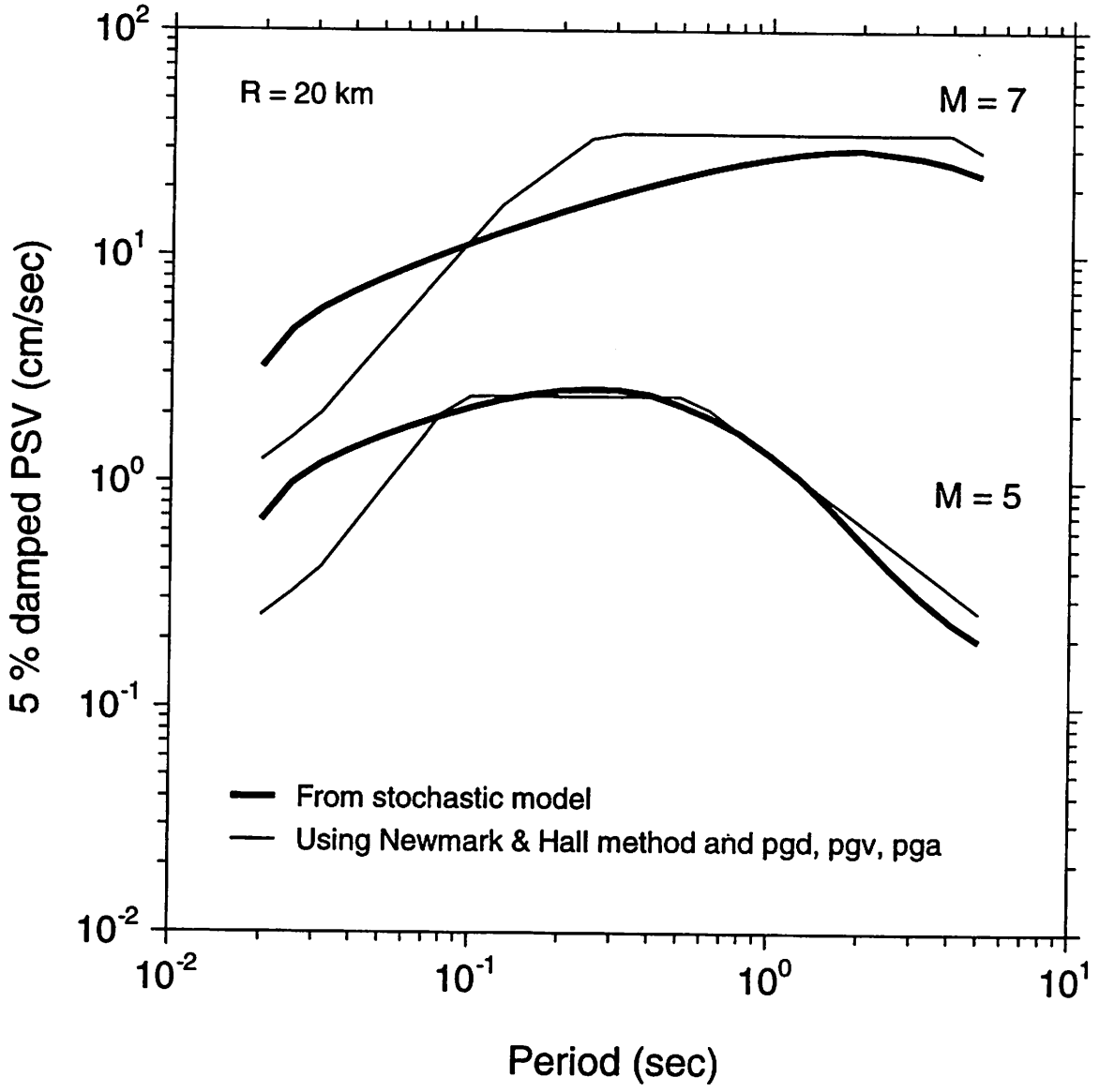

Figure 25. Pseudovelocity response spectra at 20 km as a function of oscillator period for a hard-rock site in central or eastern North America. The heavy lines give the predicted values from the stochastic model. The light lines were obtained using Newmark and Hall's median amplification factors (Newmark and Hall, 1982, Table 1), with faring to the short-period asymptote beginning at 0.125 sec and ending at 0.03 sec.

Proceedings of

ATC-35 Seminar on New Developments in Earthquake Ground Motion Estimation and Implications for Engineering Design Practice

Los Angeles, California
January 26, 1994

San Francisco, California
January 27, 1994

Seattle, Washington
February 2, 1994

New York, New York
February 9, 1994

Memphis, Tennessee
February 10, 1994

by

APPLIED TECHNOLOGY COUNCIL
555 Twin Dolphin Drive, Suite 550
Redwood City, California 94065

Funded by

U. S. GEOLOGICAL SURVEY
Reston Virginia

1994